

NATURAL RUBBER TOUGHENED POLYLACTIC ACID

Patcharaporn Somdee

A Thesis Submitted in Partial Fulfillment of the Requirements for the

Degree of Master of Engineering in Polymer Engineering

Suranaree University of Technology

Academic Year 2009

พอลิแลกติกแอซิดเสริมความเหนียวด้วยยางธรรมชาติ

นางสาวพัชราภรณ์ สมดี

วิทยานิพนธ์นี้เป็นส่วนหนึ่งของการศึกษาตามหลักสูตรปริญญาวิศวกรรมศาสตรมหาบัณฑิต
สาขาวิชาวิศวกรรมพอลิเมอร์
มหาวิทยาลัยเทคโนโลยีสุรนารี
ปีการศึกษา 2552

NATURAL RUBBER TOUNGHENED POLYLACTIC ACID

Suranaree University of Technology has approved this thesis submitted in partial fulfillment of the requirement for a Master's Degree.

Thesis Examining Committee

(Asst. Prof. Dr. Nitinat Suppakarn)

Chairperson

(Asst. Prof. Dr. Chantima Deeprasertkul)

Member (Thesis Advisor)

(Asst. Prof. Dr. Pranee Chumsumrong)

Member

(Asst. Prof. Dr. Wimonlak Sutapun)

Member

(Prof. Dr. Sukit Limpijumnong)

Vice Rector for Academic Affairs

(Assoc. Prof. Dr. Vorapot Khompis)

Dean of Institute of Engineering

พัชราภรณ์ สมดี : พอลิแลกติกแอซิดเสริมความเหนียวด้วยยางธรรมชาติ (NATURAL RUBBER TOUGHENED POLYLACTIC ACID) อาจารย์ที่ปรึกษา : ผู้ช่วยศาสตราจารย์ ดร.จันทิมา ดีประเสริฐกุล, 77 หน้า.

จุดประสงค์หลักของการศึกษานี้คือ การปรับปรุงสมบัติความเหนียวของพอลิแลกติกแอซิด (PLA) ด้วยยางธรรมชาติ (NR) เนื่องจากความสามารถในการย่อยสลายได้ตามธรรมชาติของพอลิเมอร์ทั้งสอง ทำให้พอลิแลกติกแอซิด และยางธรรมชาติเป็นที่สนใจ พอลิแลกติกแอซิด และยางธรรมชาติถูกเตรียมที่ความเข้มข้นของยางธรรมชาติต่าง ๆ จาก 0 ถึง 20 เปอร์เซ็นต์โดยน้ำหนัก ด้วยเครื่องบดผสมภายใน สมบัติทางกล สมบัติทางความร้อน และสัณฐานวิทยาของพอลิเมอร์ผสมระหว่างพอลิแลกติกแอซิดและยางธรรมชาติถูกตรวจสอบ ความต้านทานต่อการกระแทก เปอร์เซ็นต์การดึง ณ จุดขาด และความเหนียวต่อการดึงของพอลิเมอร์ผสมเพิ่มขึ้นเมื่อเพิ่มความเข้มข้นของยางธรรมชาติจนถึง 10 เปอร์เซ็นต์โดยน้ำหนัก ในทางตรงกันข้าม ความแข็งแรงต่อการดึงมีแนวโน้มลดลงด้วยการเติมยางธรรมชาติ ขณะที่ค่ามอดูลัสของยังก็ไม่เปลี่ยนแปลงอย่างมีนัยสำคัญ ค่าความต้านทานต่อการกระแทก และเปอร์เซ็นต์การดึง ณ จุดขาด ที่ปริมาตรของยางธรรมชาติ 10 เปอร์เซ็นต์โดยน้ำหนัก เท่ากับ 6.66 กิโลจูลต่อตารางเมตร และ 20.14 เปอร์เซ็นต์ ขณะที่ค่าเหล่านี้ของพอลิแลกติกแอซิดล้วน เท่ากับ 2.34 กิโลจูลต่อตารางเมตร และ 9.30 เปอร์เซ็นต์ ความเหนียวต่อการดึงของของผสมที่ 10 เปอร์เซ็นต์โดยน้ำหนักยางธรรมชาติ มีค่าเท่ากับ 609 เมกะปาสคาล ซึ่งเพิ่มขึ้นสองเท่าเมื่อเทียบกับพอลิแลกติกแอซิดล้วน เมื่อวิเคราะห์สมบัติเชิงกลพลวัต พบว่ามอดูลัสสะสม และอุณหภูมิเปลี่ยนสภาพแก้วของพอลิแลกติกแอซิดล้วน ไม่เปลี่ยนแปลงด้วยการเติมยางธรรมชาติ ขณะที่พิกแทนเจนัสสูงเสียมมีความสูงมากที่สุดที่ 5 และ 10 เปอร์เซ็นต์โดยน้ำหนักของสัดส่วนยางธรรมชาติ ซึ่งชี้ให้เห็นว่า พอลิเมอร์ผสมเหล่านี้สามารถกระจายพลังงานสอดคล้องกับผลความต้านทานต่อการกระแทกที่มีค่าสูง สัณฐานวิทยาของพอลิแลกติกแอซิดล้วน และพอลิแลกติกแอซิดผสมนี้ ถูกศึกษาโดยใช้กล้องจุลทรรศน์อิเล็กตรอนแบบส่องกราด (SEM) พบว่า พอลิเมอร์ผสมนี้เป็นแบบผสมเข้ากันไม่ได้ โดยมีอนุภาคทรงกลมของยางธรรมชาติกระจายตัวในวัฏภาคต่อเนื่องของพอลิแลกติกแอซิด ขนาดอนุภาคของยางธรรมชาติโดยเฉลี่ยมีแนวโน้มเพิ่มขึ้นด้วยการเติมยางธรรมชาติ ที่ค่าความต้านทานต่อการกระแทกสูงที่สุด ขนาดอนุภาคเฉลี่ยของยางธรรมชาติโดยปริมาตรคือ 2.30 ไมโครเมตร ผลกระทบของขนาดอนุภาคของยางธรรมชาติถูกศึกษาโดยการเปลี่ยนความเร็วรอบการหมุนของเครื่องบดผสมภายใน และความหนืดของวัฏภาคต่อเนื่องของพอลิแลกติกแอซิด ความต้านทานต่อการกระแทก และขนาดอนุภาคของยางธรรมชาติไม่เปลี่ยนแปลงอย่างมีนัยสำคัญด้วยการเปลี่ยนแปลงความเร็วรอบการหมุนจาก 40 ถึง 100 รอบต่อนาที พอลิเมอร์ผสมเมื่อใช้พอลิแลกติกแอซิดชนิดเป่าฟิล์ม (4042D) แสดงค่า

ความต้านทานต่อการกระแทกสูงกว่าชนิดที่ 3051D) ผลลัพธ์นี้บ่งบอกว่าอัตราส่วนของความหนืดมีอิทธิพลต่อความเหนียวของพอลิเมอร์ผสม สมบัติทางความร้อนของพอลิแลกติกแอซิดล้วนและพอลิแลกติกแอซิดและยางธรรมชาติผสมถูกตรวจสอบด้วยเทคนิคดิฟเฟอเรนเชียล สแกนนิ่งคาลอริเมทรี (DSC) อุณหภูมิเปลี่ยนสภาพแก้ว (T_g) อุณหภูมิการตกผลึก (T_c) และปริมาณผลึกของพอลิแลกติกแอซิดในพอลิเมอร์ผสมไม่เปลี่ยนแปลงอย่างมีนัยด้วยการเติมยางธรรมชาติ

PATCHARAPORN SOMDEE : NATURAL RUBBER TOUGHENED
POLYLACTIC ACID. THESIS ADVISOR : ASST. PROF. CHANTIMA
DEEPRASERTKUL, Ph.D., 77 PP.

POLYLACTIC ACID/ NATURAL RUBBER/ POLYMER BLENDS/ TOUGHNESS

The main objective of this study is to improve toughness properties of polylactic acid (PLA) with natural rubber (NR). Due to their biodegradability, both PLA and NR are of interest. PLA and NR were prepared at various NR concentrations from 0-20 wt% using an internal mixer. Mechanical, thermal and morphological properties of the PLA/NR blends were investigated. The impact strength, percent elongation at break and tensile toughness of the blends increase with increasing NR concentration up to 10 wt%. On the contrary, tensile strength tends to decrease with adding NR. Young's modulus did not significantly change with adding NR. At 10 wt% NR content, impact strength and elongation at break were 6.66 kJ/m² and 20.14% while these of pure PLA were 2.34 kJ/m² and 9.30%. Tensile toughness of the blends at 10 wt% NR was 609 MPa which increases two folds compared to pure PLA. By using dynamic mechanical analysis (DMA), it was found that storage modulus and glass transition temperature of PLA did not change with NR addition. At 5 and 10 wt% of NR contents, high intensity tan δ peak was obtained. It indicates that these blends can dissipate energy in consistent with the high impact strength. Morphology of pure PLA and PLA blends were examined by scanning electron microscopy (SEM). The blends are immiscible where spherical NR particles disperse in PLA matrix. The average NR particle sizes tended to increase with adding NR. At the

highest impact strength, the volume average NR particle size was 2.30 μm . Effect of NR particle size was studied by varying rotor speed of an internal mixer and viscosity of PLA matrix phase. Impact strength and NR particle size did not significantly change with varying rotor speeds from 40-100 rpm. The blends with blown film grade PLA (4042D) showed higher impact strength than injection grade (3051D). This result suggests that viscosity ratio influence toughness of the blends. Thermal properties of pure PLA and PLA/NR blends were investigated using differential scanning calorimetry (DSC). The glass transition temperature (T_g), cold crystallization temperature (T_{cc}) and crystallinity of PLA in the blends did not significantly change with adding NR.

School of Polymer Engineering

Academic Year 2009

Student's Signature_____

Advisor's Signature_____

ACKNOWLEDGEMENTS

This thesis could not successfully complete without the funding support from Suranaree University of Technology and National Center of Excellence for Petroleum, Petrochemical and Advance Materials.

First and foremost, I am deeply grateful to my thesis advisor, Asst. Prof. Dr. Chantima Deeprasertkul who gave me to feeling of the very good teacher for her teach throughout the course of this study, guidance in everything, encouragement and support. My thanks go to Asst. Prof. Dr. Nitinat Suppakarn, Asst. Prof. Dr. Pranee Chumsumrong and Asst. Prof. Dr. Wimonlak Sutapun for their constructive comments and advice given as committee members. I would like to thanks faculty and staff members of the School of Polymer Engineering and the Center for Scientific and Technological Equipment of Suranaree University of Technology for their help and suggestion. Special thanks are extended for all friends for their kindness, help and encouragement.

Finally, I owe my loving thanks and deep sense of gratitude to my parents, Mr. Pamorn and Mrs. Boason Somdee, for their loving support and encouragement me throughout the course of Master's degree at the Suranaree University of Technology.

Patcharaporn Somdee

TABLE OF CONTENTS

	Page
ABSTRACT (THAI)	I
ABSTRACT (ENGLISH).....	III
ACKNOWLEDGMENTS	V
TABLE OF CONTENTS.....	VI
LIST OF TABLES.....	X
LIST OF FIGURES	XI
SYMBOLS AND ABBREVIATIONS.....	XIV
CHAPTER	
I INTRODUCTION	1
1.1 General introduction.....	1
1.2 Research objectives	3
1.3 Scope and limitation of the study	4
II LITERATURE REVIEW	5
2.1 Miscibility of PLA/polymer blends.....	5
2.1.1 The glass transition temperature.....	6
2.1.2 Phase morphology	7
2.2 Crystallinity of PLA/polymer blends	8
2.2.1 Effect of addition of other polymers on crystallinity of PLA	9

TABLE OF CONTENTS (Continued)

	Page
2.2.2 Effect of addition of other polymers on crystallization rate of PLA.....	9
2.3 Rubber toughened polymer	10
2.3.1 Brittle to tough transition.....	10
2.3.2 Factors affecting toughness of polymer/rubber blends.....	12
2.3.2.1 Rubber content and size.....	12
2.3.2.2 Interparticle distance of disperse phase.....	14
2.3.2.3 Droplet deformation and breakup.....	17
2.3.2.3.1 Capillary number	18
2.3.2.3.2 Viscosity ratio of polymer blends.....	19
2.3.2.4 Test condition	20
2.3.2.5 Crystallinity	22
2.4 Dynamic mechanical properties of polymer blends	23
III EXPERIMENTAL METHODOLOGY	25
3.1 Materials	25
3.1.1 Polylactic acid.....	25
3.1.2 Natural rubber	26
3.2 Experimental.....	26

TABLE OF CONTENTS (Continued)

	Page
3.2.1 Sample preparations	26
3.2.1.1 Dried NR	26
3.2.1.2 PLA blends preparation	26
3.2.2 Mechanical properties.....	28
3.2.2.1 Tensile testing.....	28
3.2.2.2 Impact testing	28
3.2.2.3 Dynamic mechanical testing.....	28
3.2.3 Rheological measurement.....	29
3.2.4 Thermal properties.....	29
3.2.5 Morphology	30
IV RESULTS AND DISCUSSION.....	32
4.1 Effect of mixing temperature on physical properties and morphology of PLA blends	32
4.1.1 Mechanical properties.....	32
4.1.2 Morphology	37
4.2 Effect of rubber concentration and rubber particle size on physical properties of PLA blends	38
4.2.1 Mechanical properties.....	39
4.2.2 Thermal properties.....	41
4.2.3 Morphology	47

TABLE OF CONTENTS (Continued)

	Page
4.2.4 Dynamic mechanical properties of PLA blends	52
4.3 Effect of rotor speeds on physical properties of PLA blends	55
4.3.1 Mechanical properties	56
4.3.2 Morphology	57
4.4 Effect of viscosity ratio on physical properties of PLA blends	60
4.4.1 Mechanical properties	60
4.4.2 Morphology	62
V CONCLUSIONS	64
REFERENCES	66
APPENDICES	
APPENDIX A. RESULT OF DISTRIBUTION OF NR PARTICLE SIZE	70
APPENDIX B. PUBLICATION	72
BIOGRAPHY	77

LIST OF TABLES

Table		Page
4.1	Tensile properties of pure PLA and PLA/NR blends at mixing temperature of 200°C	37
4.2	Thermal properties of pure PLA and PLA blends with different NR contents (as obtained from DSC second heating thermograms)	44
4.3	Thermal properties of pure PLA and PLA blends with different NR contents (as obtained from DSC first heating thermograms)	46
4.4	Interparticle distance (τ) and impact strength with different NR contents	52
4.5	NR particle sizes with various rotor speeds PLA-5% and PLA-10%NR contents.....	59

LIST OF FIGURES

Figure	Page
2.1	Schematic diagram showing the brittle to tough transition of a polymer 11
2.2	Model for (surface to surface) inter-particle distance (τ) and rubber particle diameter (d)..... 15
2.3	Schematic diagram of stressed volume around a dispersed particle 16
2.4	Critical capillary number for breakup in simple shear flow. Curve was fitted to the data of Grace (1982). Sketches below the line indicate the steady drop shapes; sketches above the line show the breakup modes..... 20
3.1	Chemical structure of polylactic acid..... 25
3.2	Chemical structure of cis-1, 4-polyisoprene in Hevea latex 26
4.1	Impact strength of PLA blends with different NR contents at mixing temperature of (●)180 and (○) 200°C 33
4.2	Complex viscosity of pure PLA at mixing temperature of 180°C (●) and 200°C (○) versus angular frequency 34
4.3	Tensile stress-strain curve of the PLA blends with different NR contents at mixing temperature of 200°C 35
4.4	Mechanical properties of PLA blends as a function of NR contents: tensile moduli (●) and elongation at break (○) 36
4.5	SEM micrographs of impact fractured surface of PLA-5 wt% of NR at mixing temperature of (a) 180°C and (b) 200°C 38

LIST OF FIGURES (Continued)

Figure	Page
4.6	Tensile stress-strain curve of the PLA blends with different NR contents..... 40
4.7	Mechanical properties of PLA blends as a function of NR contents: tensile moduli (●) and elongation at break (○) 41
4.8	Tensile toughness of pure PLA and PLA blends with different NR contents 42
4.9	DSC thermograms of PLA/NR blends at heating rate of 10°C/min. Data from the second heat; (a) 0%NR, (b) 5%NR, (c) 10%NR, (d) 15%NR and (e) 20%NR 43
4.10	DSC thermograms of PLA/NR blends at heating rate of 10°C/min. Data from the first heat; (a) 0%NR, (b) 5%NR, (c) 10%NR, (d) 15%NR and (e) 20%NR 46
4.11	DSC thermograms of PLA/NR blends at cooling rate of 10°C/min: (a) 0%NR, (b) 5%NR, (c) 10%NR, (d) 15%NR and (e) 20%NR 47
4.12	SEM micrograph of PLA/NR blends in the impact testing: (a) Pure PLA, (b) PLA-1%NR and (c) PLA-3%NR (— 10µm) 48
4.12	SEM micrograph of PLA/NR blends in the impact testing: (d) PLA-5%NR, (e) PLA-10%NR, (f) PLA-15%NR and (g) PLA-20%NR (— 10µm). (continued)..... 49
4.13	NR particle size (\bar{d}_v) in PLA/NR blends with NR contents 51

LIST OF FIGURES (Continued)

Figure	Page
4.14	Storage modulus curve of pure PLA and PLA/NR blends with different NR contents 53
4.15	Tan delta curve of pure PLA and PLA/NR blends with different NR contents 54
4.16	Impact strength of PLA-5 wt% NR content with different rotor speeds 56
4.17	Impact strength of PLA-10%NR blend with different rotor speeds 57
4.18	SEM micrograph of PLA-5%NR content with various rotor speeds: (a) 40 rpm, (b) 50 rpm, (c) 70 rpm and (d) 100 rpm (— 10 μm) 58
4.19	SEM micrograph of PLA-10%NR content with different rotor speeds: (a) 40 rpm, (b) 50 rpm, (c) 70 rpm and (d) 100 rpm (— 10 μm) 59
4.20	Plot of shear viscosity, $\eta(\dot{\gamma})$ and complex viscosity, $\eta^*(\omega)$ of PLA blown film grade (\square) and injection grade (\circ) versus shear rate ($\dot{\gamma}$) and angular frequency (ω). The $\eta^*(\omega)$ data (closed symbol) were determined using SAOS with a parallel plate rheometer; the $\eta(\dot{\gamma})$ data (opened symbol) were obtained with a capillary rheometer 61
4.21	SEM micrograph of PLA/NR10 with different PLA matrix grade: (a) blown film grade and (b) injection grade (— 10 μm) 63

SYMBOLS AND ABBREVIATIONS

ω	=	Angular frequency
Ca	=	Capillary number
T_{cc}	=	Cold crystallization temperature
τ_c	=	Critical interparticle distance
Ca_{crit}	=	Critical capillary number
cm^3	=	Cubic centimeter
η^*	=	Complex viscosity
δ	=	Delta
$^{\circ}C$	=	Degree Celsius
X_C	=	Degree of crystallinity (%)
d_i	=	Diameter of particle
$\Delta H_{m,PLA}$	=	Enthalpy of fusion of PLA
$\Delta H_{c,PLA}$	=	Enthalpy of crystallization of PLA
GPa	=	Giga Pascal
T_g	=	Glass transition temperature
g	=	Gram
Hz	=	Hertz
τ	=	Interparticle distance
Γ	=	Interfacial tension
J	=	Joule
kJ	=	Kilo joule
kV	=	Kilo volt

SYMBOLS AND ABBREVIATIONS (Continued)

E'' and G''	=	Loss modulus
MPa	=	Megapascal
T_m	=	Melting temperature
μm	=	Micrometer
min	=	Minute
mg	=	Milligram
ml	=	Millilitre
mm	=	Millimeter
μL	=	Micro liter
mol	=	Mole
nm	=	Nanometer
n_i	=	Number of particle
%	=	Percent
rad	=	Radian
R	=	Radius of the drop
rpm	=	Revolution per minute
s	=	Second
$\dot{\gamma}$	=	Shear rate
η	=	Shear viscosity
E' and G'	=	Storage modulus
mm^2	=	Square millimeter
η_{NR}	=	Viscosity of natural rubber
η_{PLA}	=	Viscosity of polylactic acid

SYMBOLS AND ABBREVIATIONS (Continued)

η_d	=	Viscosity of disperse phase
η_m	=	Viscosity of matrix phase
η_r	=	Viscosity ratio
\bar{d}_v	=	Volume average particle size
ϕ	=	Volume fraction of rubber
wt	=	Weight
\bar{d}_w	=	Weight average particle size
x_{PLA}	=	Weight fraction of PLA in blend
ACM	=	Acrylic rubber
BTT	=	Brittle to tough transition
DSC	=	Differential scanning calorimetry
DMA	=	Dynamic mechanical analysis
DMTA	=	Dynamic mechanical thermal analysis
EPDM	=	Ethylene-propylene-diene monomer
FTIR	=	Fourier transform infrared spectroscopy
MDSC	=	Modulated differential scanning calorimetry
NR	=	Natural rubber
PLA	=	Poly(lactic acid)
PLLA	=	Poly(L-lactic acid)
PDLLA	=	Poly(D,L-lactic acid)
PBSA	=	Poly(butylene succinate adipate)
PBS	=	Poly(butylene succinate)
PBAT	=	Poly(butylene adipate-co-terephthalate)

SYMBOLS AND ABBREVIATIONS (Continued)

PCL	=	Poly(ϵ -caprolactone)
PES	=	Poly(ethylene succinate)
PVB	=	Poly(vinyl butyral)
PVDF	=	Poly(vinylidene fluoride)
PMMA	=	Poly(methyl methacrylate)
PBA	=	Poly(<i>n</i> -butyl acrylate)
PET	=	Poly(ethylene terephthalate)
PP	=	Polypropylene
PTT	=	Poly(trimethylene terephthalate)
SEM	=	Scanning electron microscopy
TPS	=	Thermoplastic starch
TEM	=	Transmission electron microscope

CHAPTER I

INTRODUCTION

1.1 General introduction

Presently, environment of all over the world is contaminated with solid waste pollution. One way to solve problem of solid waste from polymer is replacing commodity synthetic polymer with biodegradable polymers (Huang, 1985). Polylactic acid (PLA) is biodegradable polymer that has been widely used in an industrial application.

PLA is a biodegradable aliphatic polyester, produced from renewable resources. It has received much attention in the research of the alternative biodegradable polymers. Commercial PLA is synthesized by ring opening polymerization of lactides which are the cyclic dimers of lactic acids. These lactic acids can be obtained from fermentation of renewable resources, the fermentation of crop like corn starch and sugar feed stocks etc. (Lunt, 1998). PLA has been found to be environmentally biodegradable through a two-step process that begins with the high molecular weight polyester chains hydrolyzing to lower molecular weight oligomers under an appropriate temperature and moisture environment. In the second step, microorganisms convert these lower molecular weight components to carbon dioxide, water and humus. Commercial PLA grades are copolymers of poly (L-lactic acid), noted PLLA, and poly (D,L-lactic acid), noted PDLLA, which are produced from L-lactides and D, L-lactides, respectively. The ratio of L- to D, L-enantiomer is known to affect the properties of the polymer obtained, such as melting temperature

and degree of crystallinity (Vert, Schwach, and Coudane, 1995). Standard PLA has high modulus (3 GPa) and strength (50-70 MPa) comparable to many petroleum-based plastics, but is brittle. For wide applications, brittle PLA is improved by several techniques. Blending is a common method to improve properties of polymer. Brittleness of PLA can be modified by blending with other materials.

Polymer blending is a method for obtaining properties that the individual do not possess and has been widely used also for lactic acid based polymer. Blending of PLA with other polymers offers the possibility of changing for example the degradation rate, permeability characteristics, drug release profiles, thermal and mechanical properties. Examples of biodegradable polymer used to blend with PLA are poly (butylenes succinated adipate) (PBSA) (S. Lee and J. W. Lee, 2005), poly (butylene adipate-co-terephthalate) (PBAT) (Jiang, Wolcott, and Zhang, 2006), poly (ϵ -caprolactone) (PCL) (Todo, Park, Takayama, and Arakawa, 2007) and poly (ethylene succinate) (PES) (Lu, Qiu, and Yang, 2007) etc. Blending PLA with elastomeric disperse phase is one technique to improve toughness of PLA.

Toughness is a measure of resistance to fracture. It is an important requirement in most loads bearing application of materials. In order to achieve the desired properties, the polymer blends should in general be miscible therefore phase separation in the blends do not occur. Immiscible blends are, however, preferred when rubber toughening of PLA is desired. Many of the PLA blends that have been studied are immiscible or only partly miscible and may require some sort of compatibilizer in order to make them miscible. The goal of such techniques is to combine the stiffness and processability of brittle polymer matrix with the fracture resistance of elastomers. Rubber is normally used to improve toughness of brittle polymer. The main parameter

that influences toughness of the blends is rubber phases such as rubber content, rubber size (Li, Iwakura, Zhao, and Shimizu, 2008) and interparticle distance (Margolina and Wu 1988; Wu, 1990; Jiang, Tjong, and Li, 2000; W. Jiang, Yu, and B. Jiang, 2004).

Natural rubber (NR) has been widely used to improve toughness of polymer. Besides its high fracture resistance, NR is biodegradable and can be obtained from renewable resources. Natural rubber latex is obtained from *Hevea brasiliensis* tree. The polymer is a highly linear cis-1,4-polyisoprene of about 5×10^5 g/mol which is unable to crystallize under normal conditions. It owes its colloid stability to the presence of adsorbed proteins at the surface of the rubber particles. Rubber particles varied in size from 0.15 μm to 3 μm (Krocshowitz and Jacqueline, 1990). The fresh latex is not utilized in its original form due to its high water content and susceptibility to bacterial attack. It is necessary both to preserve and concentrate the latex, so that the natural rubber latex is stable and contains 60% or more of rubber. These adsorbed proteins are in the anionic state, so that the rubber particles carry negative charges at their surfaces (Blackley, 1987).

1.2 Research objectives

The main objective of this study is to improve toughness properties of PLA with NR. In order to obtain toughened PLA, effects of rubber contents, mixing conditions and viscosity ratio on mechanical, thermal and morphological properties will be investigated.

1.3 Scope and limitation of the study

In this study, NR was used to blend with PLA. The effect of NR on mechanical properties, thermal properties, dynamic mechanical properties and morphology of the blends were investigated. Natural rubber latex was dried before use. Blends of PLA and NR at the compositions 0, 1, 3, 5, 10, 15 and 20 wt% NR were prepared using an internal mixer and compression molding. Effects of mixing conditions which are rotor speed and temperature were explored. Mechanical and thermal properties were investigated by tensile testing, impact testing and differential scanning calorimetry, and dynamic mechanical test. Morphology of the blends was studied using scanning electron microscopy technique.

CHAPTER II

LITERATURE REVIEW

Polylactic acid is biodegradable polymer which has become significantly important material in the present. To overcome its brittleness, PLA was blended with other materials to improve toughness of PLA. Many factors were considered for improving PLA blend properties such as miscibility of PLA blend, crystallinity of PLA blend, toughness of polymer blends, rheological properties and general properties of domain phases.

The objective of this study is to improve toughness properties of PLA by blending with NR. In previous work, PLA/biodegradable and PLA/nonbiodegradable polymer blends have been considered to improve the mechanical properties and morphologies of blends, specifically toughness properties. Relationship between physical properties and morphology of the PLA/NR blend were made.

2.1 Miscibility of PLA/polymer blends

PLA was blended with various polymers to improve the properties of PLA. PLA blends were found to be either miscible or immiscible. Miscibility of polymer blend influences properties of the blends such as thermal properties, mechanical properties and physical properties. Miscibility of polymer blends can be characterized by differential scanning calorimetry (DSC), scanning electron microscopy (SEM), transmission electron microscope (TEM) and Fourier transform infrared spectroscopy

(FTIR) etc. The glass transition temperature and phase morphology are typically determined to indicate miscibility of polymer blends.

2.1.1 The glass transition temperature

Many researchers have studied behavior of glass transition temperature on both PLA/nonbiodegradable and PLA/biodegradable polymer blends. In the case of miscible blends, a result from DSC analysis shows single glass transition temperature (T_g). Partial miscibility of PLA blends was also observed where two glass transitions temperatures were detected at temperatures differing from the corresponding T_g of the components. The T_g of the polymer with the lower glass transition temperature increases and, conversely, the T_g of the polymer with the higher glass transition temperature decreases, thus shortening the temperature interval between the two glass transitions. The extent of this shortening is a measure of miscibility. Polylactic acid (PLA) and poly (butylene succinate) (PBS) are such biodegradable polymers which are aimed to replace commodity polymers in future applications. The blends were investigated by modulated differential scanning calorimetry (MDSC). The glass transition temperature of PLA did not much change with the addition of PBS, but for PLA/PBS blend of 80/20 composition there is partial miscibility between the two polymers (Bhatia, Gupta, Bhattacharya, and Choi, 2007). A binary blend of PLA and poly (butylene succinate adipate) (PBSA) was investigated. DSC thermograms of blends indicated that the thermal properties of PLA did not change noticeably with the amount of PBSA. The glass transition temperatures of the PBSA and the PLA were about -45°C and about 63°C , respectively. A direct proof of polymer miscibility in blend can be obtained by observing the behavior of the T_g of blends. T_g decreased from 63°C for pure PLA to

59°C for blend containing 80 wt% PBSA due to interaction between PLA and PBSA chains (S. Lee and J. W. Lee, 2005).

The existence of glass transition temperature of each component in the blends indicates immiscibility. Biodegradable polylactide/poly (butylene adipate-co-terephthalate) (PBAT) blends are immiscible with the glass transition temperatures remain unchanged with varying PBAT concentrations, indicating the lack of significant molecular interactions between PLA and PBAT (Jiang *et al.*, 2006). Polylactic acid and poly (vinyl butyral) (PVB) blend were investigated. PVB was prepared by reacting poly (vinyl alcohol) with butyral aldehyde in acidic medium. PLA was blended with PVB through solution casting method using chloroform as the common solvent. The DSC results showed that the glass transition temperature of the PLA and PVB remained more or less constant with the composition of the blend. The existence of two glass transition temperatures in the blends indicated that PLA and PVB were immiscible over the composition range investigated. FTIR spectra did not appreciably change with respect to blend composition, implying the immiscibility of the two polymers (Khurma, Rohindra, and Devi, 2005). The blends of poly (L-lactide) and poly (ethylene succinate) (PES) were studied. Both polymers are biodegradable semicrystalline polyesters. DSC results of PLLA/PES blend showed T_g and T_m of both components, suggesting the immiscibility between two phases (Lu *et al.*, 2007).

2.1.2 Phase morphology

Morphology of the immiscible blends typically shows a sea and island structure. Partial miscibility of the dispersed phase with the matrix can bring about many property changes, including tensile and impact properties such as in PLA/PBSA

system (S. Lee, and J. W. Lee, 2005). In the case of PLA/PBAT, blend shows immiscible phase morphology with the PBAT evenly dispersed in the form of 300 nm domains within PLA matrix. Furthermore, SEM micrograph showed debonding of the round domain particles in the PLA matrix. Cavities were enclosed around PBAT particles that can be explained by the debonding of PBAT particles on PLA matrix (Jiang *et al.*, 2006). SEM micrographs of the cryo-fracture surfaces of PLLA/poly (ϵ -caprolactone) (PCL) blend were investigated. It is clearly seen that the size of PCL phases increased with PCL content. It is also seen that voids are created as a result of drop of the dispersed PCL phases. PLLA/PCL blends created macro-phase separation of the two components due to difference of solubility parameter (Todo *et al.*, 2007).

2.2 Crystallinity of PLA/polymer blends

Disadvantages of poor mechanical properties and slow crystallization rate of PLA limit its wide application. Pure PLA shows slow crystallization rate and low degree of crystallinity. Thus adding nucleating agent or slow cooling process is applied to PLA crystallization. However, blending with some polymers has shown the improvement of crystallization rate and degree of crystallinity of PLA. Degree of crystallinity of PLA blends can be characterized using DSC technique. Equation (3.1) (as shown in Chapter three) is used to determine percentage of crystallinity (X_C) of PLA in the blends (Khurma *et al.*, 2005; Lu *et al.*, 2007).

In general, degree of crystallinity influences mechanical properties of PLA blends. With higher degree of crystallinity, modulus and strength of PLA blends increase.

2.2.1 Effect of addition of other polymers on crystallinity of PLA

Addition of one polymer to another can affect the thermodynamics and kinetics of crystallization of either component. Thus the degree of crystallinity is changed. In the case of PLLA/PCL blends, degree of crystallinity of PLA tended to increase with PCL content. The result of DSC thermograms of PLLA/PCL blends showed enlargement of the PLLA crystallization temperature peak. It suggests that the crystallization of PLLA is activated by PCL blending (Todo *et al.*, 2007). Degree of crystallinity did not change. It indicated that the addition of PCL had no interaction with PLA. In the case of PLA/PVB blends, adding PVB had no contribution in decreasing degree of crystallinity of PLA. Furthermore, mechanical analysis showed that the tensile strength and percent elongation decreased when PVB content increase due to no interaction of H-bonding between PLA and PVB (Khurma *et al.*, 2005).

2.2.2 Effect of addition of other polymers on crystallization rate of PLA

The crystallization rate of PLA was accelerated with some polymer but it had little effect on degree of crystallinity of PLA. In the case of PLA/PBAT blends, PBAT component accelerated the crystallization rate of PLA but had little effect on its degree of crystallinity. The addition of PBAT greatly increased the crystallization rate of PLA. At the heating rate of 5°C/min as given enough time to complete crystallization, both neat PLA and PLA in blend crystallize to the same degree of crystallinity. Therefore, adding PBAT did not increase the degree of crystallinity of the PLA in the blends. With the increase in PBAT content (5-20 wt%), tensile strength and modulus decreased. Though, elongation at break and toughness were dramatically increased (Jiang *et al.*, 2006). PLLA/PES blends were investigated. The

crystallization rate of PLLA at 100°C was accelerated with the increase of PES in the blends while the degree of crystallinity of PLLA did not change (Lu *et al.*, 2007). Adding other polymers might nucleate and grow PLA crystals, resulting in high crystallization rate without the change in degree of crystallinity.

2.3 Rubber toughened polymer

Toughness is a measure of resistance to fracture. It is an important requirement in most loads bearing application of materials. There are many techniques to enhance toughness of brittle polymers. Among them, blending the brittle matrix with elastomeric disperse phase is the most commonly used. Combined the stiffness and processability of brittle polymer matrix with the fracture resistance of elastomers would be expected.

The manner in which toughened polymers fail depends on both intrinsic and extrinsic factors. However, the rubber phase intended for rubber toughening must be dispersed as small particles in the plastic matrix. The optimum particle size and size distribution of the dispersed particles are required. Too small or too large rubber particles could not promote toughening (Walker and Collyer, 1994).

2.3.1 Brittle to tough transition

The brittle to tough transition of polymers has been the subject of interest for the polymer scientists. The brittle to tough transition (BTT) of the polymers can be clearly seen from the schematic diagram, as shown in Figure 2.1. The regions 1, 2 and 3 in this diagram correspond to brittle, transition and tough regimes, respectively. The parameter X denotes the temperature, rubber content, strain rate, etc. The critical value of X_C is a value at which BTT occurs (Jiang *et al.*, 2000).

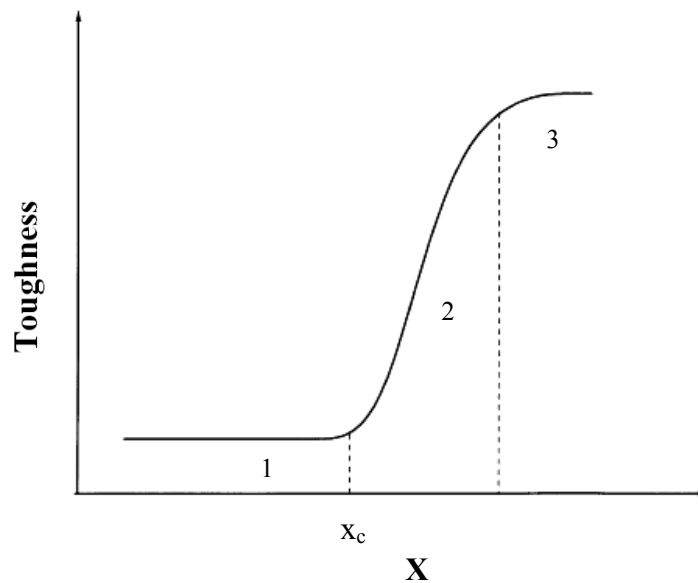


Figure 2.1 Schematic diagram showing the brittle to tough transition of a polymer.

Some studies showed that the maximum toughness could be obtained at the optimum value of the parameter, not as the critical transition shown above. For example, PLA blended with PBSA showed the highest impact strength at 10-20 wt% of PBSA. Lower and higher than that contents the impact strength was small (S. Lee and J.W. Lee, 2005). A rubber particle size gives a maximum toughness for an optimum particle size when rubber content and interfacial adhesion were fixed. The optimum rubber particle size depends on the entanglement density (v_e) of matrix. The optimum particle size decreases with increasing v_e and the matrix become more ductile (Walker and Collyer, 1994).

2.3.2 Factors affecting toughness of polymer/rubber blends

Many factors e.g. the molecular weight, the crystallinity of the matrix, the rubber contents, the interparticle distance, the particle size and the interfacial characteristics play important roles in level of toughening.

2.3.2.1 Rubber content and size

Effect of rubber concentration and particle size as well as size distribution influences properties of the blends. Generally, increasing the concentration of rubber phase decreases the blend modulus and tensile strength irrespective of whether the matrix is brittle or pseudo ductile. The critical/optimum particle size and distribution for toughening depends on the type of matrix and rubber as well as the rubber concentration. A crazing mechanism is better suited to a higher particle size than a shear yielding mechanism. In addition, the optimum size distribution of the dispersed phase depends on the preferred deformation mechanism of the matrix. With highly distributed, the rubber phase can act as an effective stress concentrator and enhances both crazing and shear yielding in the matrix. The preferred deformation mechanism whether crazing or shear yielding is dominant depends on the intrinsic toughness of the matrix and morphology of the blends (Walker and Collyer, 1994).

Rubber particle size over 5 microns is often too large to interact with the stress field at the crack tip while rubber particle size under 100 nm is too small to cavitate effectively. Rubber phases dispersed in polymer matrix with most particle size of less than 100 nm are so called nanodomains. Without the cavitation of the rubber particles, subsequent matrix shear banding in the presence of a triaxial

stress field at crack tip is very unlikely (Walker and Collyer, 1994; Li *et al.*, 2008). In the case of polymer/rubber blends, morphology and properties of poly (vinylidene fluoride) (PVDF)/acrylic rubber (ACM) blends with very minor ACM content (less than 10 wt%) were investigated. By simply blending PVDF with several ACM contents, ACM was dispersed in the PVDF phase with particle size of less than 100 nm. The impact strength increased with increasing the ACM content with pertaining PVDF modulus (Li *et al.*, 2008). The blends with the ACM domains size of less than 100 nm in PVDF matrix shows markedly increased elongation at break. It is obvious that the widely used cavitation toughening mechanism did not apply for PVDF/ACM blend. Effect of particle size and rubber content on impact strength of poly (methyl methacrylate) (PMMA) and poly (*n*-butyl acrylate) (PBA) blends were studied. The relationship between the impact strength and rubber particle size is represented by a bell shaped curve where toughness is maximum at an optimal rubber particle size. The optimum particle size is around 0.25 μm irrespective of rubber content. The impact strength was reported as a function of the rubber content. The impact strength increases up to a certain (around 12 wt%) level of rubber content and decreases above that level. The decrease of toughness above a certain rubber phase content is related to the decrease of the modulus and yield stress. If blends have a low modulus and low yield stress, the stress cannot be transferred far from the crack tip. This results in a decrease of the stress whitening zone and the toughness (Cho, Yang, and Park, 1998). In poly (ethylene terephthalate) (PET) toughened by natural rubber (NR), when NR content is increased, the impact property increases while the Young's modulus decreases. This result may be due to the elastomeric nature of NR. The brittle transition is modified by the presence of rubber dispersive phase. This phase

can absorb and dissipate the crack energy produced. This prevents the abrupt breaking of the specimen. By increasing rubber concentration, the acceptors of dissipation energy are increased. When NR content is increased, Young's modulus decreases. This was most likely due to factors such as the elastomeric nature of NR in PET/NR blend (Phinyocheep, Saelao, and Buzaré, 2007). In the case of biodegradable blends, PLA/PBAT blends were investigated. Melt elasticity and viscosity of the blends increased with adding PBAT. Adding PBAT (5-20 wt%), tensile strength and modulus of the blends decreased while elongation and toughness dramatically increased. Adding PBAT could change the failure mode from brittle fracture of pure PLA to ductile fracture of the blends. SEM micrographs of the impact fractured surfaces show more evidences of ductile fracture as more and longer fibrils can be observed from the surface with increase in PBAT content. Cavitation caused by debonding can be clearly identified. The large voids in fracture surface might be formed by the coalescence of neighboring small cavities (Jiang *et al.*, 2006). In the case of PLLA/PES blends, the mechanical properties of the blends were examined by tensile testing. Percent elongation at break increases when adding PES, while Young's modulus was still kept constant. Fracture behavior of PLLA/PES is the same as PLA/PBAT blends. SEM micrograph revealed smooth surface of PLLA, while PES presented a rough surface. The smooth fracture surface indicated the brittle fracture behavior of neat PLLA, while the rough surface implied the ductile fracture behavior of neat PES. For PLLA/PES blends, the surface changed from smooth to rough with increasing PES content (Lu *et al.*, 2007).

2.3.2.2 Interparticle distance of disperse phase

Wu proposed a significant parameter that dominates the brittle to tough transition of polymer/rubber blends is interparticle distance (τ), as shown in Figure 2.2. According to Wu, the tough polymer blends can be obtained if τ is smaller than a critical interparticle distance (τ_c). This can be valid only if the blends dissipate impact energy mainly by increased matrix yielding. By using a series of rubber modified nylon 6, 6 regardless of particle size and rubber concentration, τ_c depends only on matrix properties. Based on Wu's model (Wu, 1985), τ relates with two parameters, weight average particle size and volume fraction of rubber, presented in equation (2.1).

$$\tau = \bar{d}_w \left[\left(\frac{\pi}{6\phi} \right)^{1/3} - 1 \right] \quad (2.1)$$

τ : an interparticle distance

\bar{d}_w : a weight-average particle size

ϕ : a volume fraction of rubber

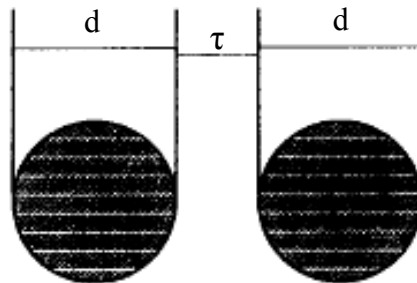


Figure 2.2 Model for (surface to surface) interparticle distance (τ) and rubber particle diameter (d).

As the elastic modulus of the dispersed phase is different from that of the matrix, when a force is applied to a sample of the polymer blend a stress concentration will form around particles of the dispersed phase. Its scope can be described as a stressed volume, in which the diameter of the stressed volume $S = \tau + d$, where d is the diameter of the dispersed particle and τ is the interparticle distance (Wu, 1990; Margolina and Wu, 1988), as shown in Figure 2.3. There are many experimental and theoretical results which confirm that, during impact or tensile fracture of polymer blends, the rubber particles will be greatly deformed until cavitation of the rubber particles occurs. This leads to shear yielding propagating through matrix ligaments thus the polymer blend is tough (W. Jiang, Liang, and B. Jiang, 1998).

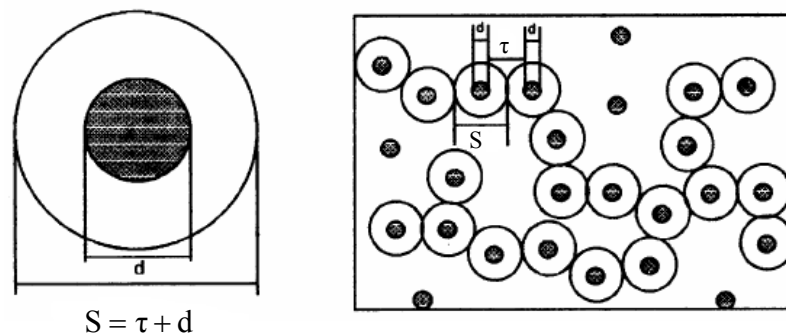


Figure 2.3 Schematic diagram of stressed volume around a dispersed particle.

Several authors have used Wu's model to study the toughening behavior of polymers. However, it was found that the τ_c not only depends on the matrix materials but also depends on the properties of the dispersed phase. Critical interparticle distance is defined from plotting the impact strength as a function of the

interparticle distance at which impact strength suddenly decreases. Arostegui, Gaztelumendi, and Nazabal (2001) studied the relation between the moduli of the matrix and the rubbery dispersed phase. Result showed that τ_c decreased as the modulus of elasticity of matrix increased (Arostegui, Gaztelumendi, and Nazabal, 2001). It was found that for poly (trimethylene terephthalate) (PTT)/poly (ethylene-octene) copolymer (mPEO) blend, τ_c depended on the modulus of elasticity of the dispersed phase, and it increased rather linearly as rubber modulus (Guerrica-Echevarra *et al.*, 2007). Contradict to Wu, Jiang *et al.* (2004) revealed that the matrix properties does not affect τ_c in PP/rubber blend. The notched Izod impact strength of the PP (more than 25 J/m) is higher than that of the nylon 66 (18.6 J/m) but the τ_c for PP/rubber blends (0.15 μm) is smaller than that for the nylon 66/rubber blends (0.30 μm). Therefore, the toughness of matrix polymer should not be a key parameter that determines value of critical interparticle distance (Jiang *et al.*, 2004). Previously studied, the brittle to tough occurred when τ of disperse phases smaller than τ_c by matrix yielding dominates. In the case of PLA/NR blends, NR particles disperse in PLA matrix phase influence toughness of the blends. Therefore, interparticle distance of NR particle was examined by equation (2.1) or (3.3).

2.3.2.3 Droplet deformation and breakup

Einstein (1906) studied the viscosity of hard spheres on dilute suspension in Newtonian liquid, to dispersion of the single Newtonian liquid droplet in another Newtonian liquid. Twenty years later, Taylor (1932; 1934) extended the work of Einstein. The breakup of a single Newtonian drop in a simple shear field was investigated. When the radius of the drops is great enough or the rate of distortion is high, the drops will breakup. Taylor derived equation of drop breakup using viscosity

ratio (η_r), viscosity of disperse phase (η_d)/viscosity of matrix phase (η_m), and capillary number (Ca).

2.3.2.3.1 Capillary number

The capillary number is the ratio between the deforming stresses (matrix viscosity times shear rate) imposed by the flow and the interfacial force following equation (2.2), where η_m is viscosity of matrix phase, $\dot{\gamma}$ is the shear rate, R is the radius of the drop and Γ is the interfacial tension.

$$Ca = \frac{\eta_m \dot{\gamma} R}{\Gamma} \quad (2.2)$$

If Ca is small, the interface forces dominate and the steady drop shape develops. If Ca exceeds a critical value (Ca_{crit}), the drop becomes unstable and finally breaks. Taylor predicted that the droplet breakup occurs when the flow-induced deformation, D as shown in equation (2.3) reaches approximately 0.5.

$$D = Ca [(19\eta_r+16) / (16 \eta_r+16)] \approx 0.5 \quad (2.3)$$

Taylor also demonstrated experimentally that for value of η_r from 0.1-1, droplets breakup. Equation (2.3) indicates that the viscosity ratio, the shear stress and the interfacial tension are critical variables in controlling particle deformation and breakup in Newtonian fluids.

2.3.2.3.2 Viscosity ratio of polymer blends

The viscosity ratio is the most critical variable for controlling blend morphology. Generally, if the minor component has a lower viscosity than the major one, the minor component will be finely and uniformly dispersed. On the other hand, the minor component will be coarsely dispersed if its viscosity is higher than that of the major component. It is generally believed that the viscosity ratio should be approximately unity when designing new polymer blends. Wu (1987) has shown that the dispersed rubber phase in rubber and polyamide blends can break up during twin-screw extrusion even when $\eta_r < 4$. Wu suggested that as the viscosity moves away from unity in either direction, the dispersed particles become larger. It is clear from both experiments and Taylor's theory that under conditions of steady breakup in shear flow, a lower viscosity ratio results in finer dispersed-particle size. When a droplet is suddenly subjected to flow it will deform, orient, and possibly break up. The droplet response is determined by its viscosity ratio, by the capillary number, and by the nature of the flow (shear versus elongation). For capillary numbers less than a critical value the droplet attains a steady shape and orientation, whereas above the critical capillary number the droplet eventually breaks up. The critical capillary number versus η_r for single Newtonian droplets was measured by Grace (1982), in both simple shear and planar elongation, by gradually increasing the strain rate until breakup. Figure 2.4 summarizes the results in simple shear flow, indicating that no breakup is possible when $\eta_r > 4$.

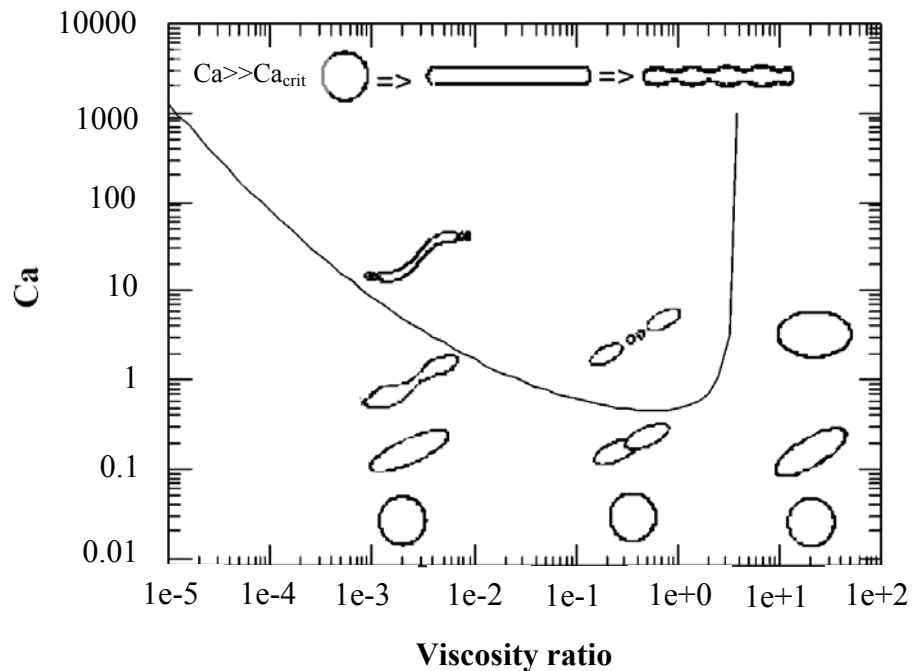


Figure 2.4 Critical capillary number for breakup in simple shear flow. Curve was fitted to the data of Grace (1982). Sketches below the line indicate the steady drop shapes; sketches above the line show the breakup modes.

2.3.2.4 Test condition

The notched impact strength of polymer matrix increases dramatically when the temperature exceeds brittle to tough transition temperature or glass transition temperature of the polymer matrix. The values of inter-particle distance can be calculated by Wu's model. From equation (2.1) or (3.3), as the rubber volume fraction moves toward zero, namely, for pure matrix without rubber phase, τ approaches infinity. The toughness of PP/EPDM was measured over a wide range of temperature (25-132°C) and rubber composition (0-26 wt%). The notched Izod impact strength of PP can be improved by increasing temperature or adding EPDM rubber, the decreasing τ if the particle size did not change (0.47 μm). Increasing

temperature and decreasing interparticle distance have equivalent effect on brittle to tough transition of toughening PP with EPDM. τ_c increases with increasing temperature and increases suddenly when the temperature is close to T_g of pure PP (Jiang *et al.*, 1998).

The effect of interparticle distance and tensile speed on the brittle to tough transition of PP/EPDM blends were studied. The toughness of the blends was determined from the tensile fracture energy of the side-edge notched samples. A sharp brittle to tough transition was observed in the fracture energy versus interparticle distance curves when the crosshead speed < 102.4 mm/min. The result showed that the brittle to tough transition of PP/EPDM blend occurred by reducing τ or decreasing the tensile speed (Jiang, Tjong, and Li, 2000). In the case of screw rate, poly (trimethylene terephthalate) and poly (ethylene octene) blends was investigated. The larger particle size of PTT/mPEO blends compared with that obtained in PET/mPEO blends is attributed to the lower viscosity of the PTT matrix. After increasing the screw rate, the dispersed particle size decreased. The consequent decrease in interparticle distance was enough to lead to impact strength values typical of super-toughness (15-fold that of the matrix) at mPEO contents above 25 wt%. At 30 wt% rubber content the decrease in modulus was approximately 23% (Guerrica-Echevarra *et al.*, 2007).

The effect of physical aging on properties of poly (L-lactide) (PLLA) was studied. The effect of physical aging on mechanical properties was explained from the viewpoint of the rearrangement of polymer chains. PLLA specimens both aged and unaged were investigated. The mechanical properties of PLLA are significantly dependent on the thermal history. The un-aged PLLA

specimen can elongate to 300% of its original length. Besides, the neck is formed during tensile deformation of the un-aged sample, that it is ductile and flexible. The morphology of the fracture surface was estimated using SEM after the tensile test. Fracture surface of PLLA changed from the “ductile” to “inductile” manner during physical aging. Un-aged sample showed the fracture surface with the long ridges and valley relief which are parallel to the film plane and perpendicular to the stress direction. This is characterized as a ductile material with high toughness. Fibrils of the oriented polymer, which are the remnants of crazes are observed. These signify that the un-aged PLLA is more ductile, which undergoes the crazing and fibrillation process in the tensile deformation. In the case of aged sample, the surface is relatively flat and has lost its orderly ridges and valley relief. Moreover, large cracks or cavities are present in the surface. These indicate the failure of aged PLLA under tensile loadings is mainly in the “brittle” manner (Pan, Zhu, and Inoue, 2007).

2.3.2.5 Crystallinity

For PP/EPDM blending, the brittle to ductile transition temperature increases with increasing crystallinity. In the case of brittle fracture, the fracture energy decreases with increasing crystallinity. In the case of ductile fracture, the fracture energy seems to remain constant. Ductile deformation is due to pronounced plastic deformation during crack propagation. Plastic deformation occurs when the yield stress drops below the fracture stress. With increasing crystallinity, the fracture stress increase slightly while the yield stress increases strongly. The overall effect of crystallinity is an increase in yield stress in relation to the fracture stress, resulting in an increase in brittle to ductile transition temperature with increasing crystallinity (Van de Wal, Mulder, and Gaymans, 1999).

2.4 Dynamic mechanical properties of polymer blends

Generally, dynamic mechanical analysis (DMA) measures stiffness and damping of material, reported as modulus and $\tan \delta$. The storage modulus (E' or G') is the measure of the sample's elastic behavior but not the same as Young's modulus. The loss modulus (E'' or G'') is the measure of the viscous response of material. The ratio of the loss to the storage modulus is the $\tan \delta$ and is often called damping. Damping is a measure of energy dissipation of material. It is the dissipation (loss) of energy in a material under cycle load. It is a measure how well a material can get rid of energy and is reported as tangent of the phase angle ($\tan \delta$). This damping indicates how good a material will be at absorbing energy. The glass transition from DMA is seen as a large drop in the storage modulus. Glass transition temperature (T_g) indicates the relaxation in a polymer where a material changes from a glassy to a rubbery state. Martin and Av erous (2001) investigated PLA melt blended with thermoplastic starch (TPS) using DMA. The blends showed two distinct T_g s which varied toward the T_g of TPS with the blend composition, indicating some degree of interaction. The influence of a plasticizer on the storage modulus and dissipation factor of the PLA was investigated. The DMA curve of pure PLA shows a marked drop in E' and a sharp $\tan \delta$ peak around 67°C , corresponding to the glass transition. The rise of E' around 100°C is due to crystallization. Above T_g , the increase of chain mobility favors the crystallization process, at a slow scan rate ($1.5^\circ\text{C}/\text{min}$). The DMA run of pure PLA at around 125°C (at the maximum of the E' rise), the crystallinity reached up to 29%. Then, E' drops again as the material starts to flow when increasing temperature. The DMA curves of plasticized PLA are of similar shape. The modulus drop associated with the T_g of plasticized PLA decreases almost linearly with

increasing plasticizer concentration. Moreover, the height of $\tan \delta$ peak decreases. This phenomenon can be explained in terms of the degree of crystallinity. The amorphous PLA shows a very sharp and intense peak because there is no restriction to the chain motion, whereas the crystallinity of plasticized PLA test samples hinder the chain mobility, resulting in the reduction of sharpness and height of $\tan \delta$. The rise of E' , due to crystallization, still proceeds for the plasticized PLA test bars, but at lower temperatures than for pure PLA. Pan *et al.* (2007) studied effect of physical aging (annealing) on the enthalpy relaxation of PLLA. Dynamic mechanical thermal analysis (DMTA) showed increasing in E' and E'' curves above glass transition appears between 100 and 140°C. The result attributed to the cold crystallization occurring in this temperature range during heating. The E' increases with aging. Both the widths of E'' and $\tan \delta$ peaks decrease with aging. According to the theory of Fox and Flory, this observation can be attributed to the decreasing in amount of free volume with aging. The drop of ductility in physical aging is correlated to the rearrangement of polymer chains in physical aging. As for polymer above T_g , owing to the larger free volume, the chains possess more mobility. Accordingly, the arrangement of polymer chains is more irregular and free. Because of the more irregular arrangement of polymer chains, in the un-aged PLLA some chains are possibly twisted and interlaced with each other. Therefore, the un-aged PLLA is likely to possess a relatively disordered chains arrangement. In the aging process, because of the reduction of free volume, the polymer chains will rearrange from a loose packing of the quenched polymer toward more dense chain packing.

CHAPTER III

EXPERIMENTAL METHODOLOGY

In this chapter, the experimental details on PLA/NR blend preparation and tests for mechanical, thermal and rheological properties were described. Morphology analysis of the blends was also studied.

3.1 Materials

3.1.1 Polylactic acid

Two commercially available polylactic acid (PLA) grades (PLA 4042D and 3051D) were purchased from NatureWorks. The density of both grades is 1.24 g/cm³. As determined from differential scanning calorimetry (DSC) analysis, PLA 4042D exhibits a glass transition temperature (T_g) and a melting temperature (T_m) of 52.14°C and 146.68°C, respectively. Chemical structure of PLA is shown in Figure 3.1.

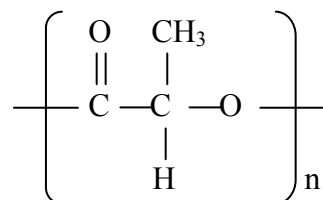


Figure 3.1 Chemical structure of polylactic acid.

3.1.2 Natural rubber

High ammonia natural rubber (NR) latex was purchased from Thai Hua Rubber Public Company Ltd., Thailand (Udonthani). NR latex has 60% dry rubber content, exhibits a density of 0.93 g/cm^3 at 20°C and a glass transition temperature around -72°C . Chemical structure of cis-1, 4-polyisoprene is shown in Figure 3.2.

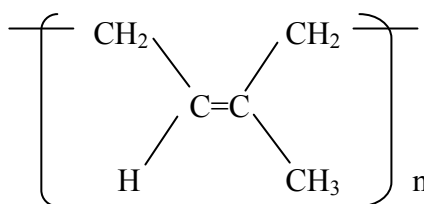


Figure 3.2 Chemical structure of cis-1, 4-polyisoprene in Hevea latex.

3.2 Experimental

3.2.1 Sample preparations

3.2.1.1 Dried NR

Dry natural rubber was prepared from NR latex. White turbid liquid latex was poured onto Petri dishes and dried in an oven at 70°C for three days. The yellowish NR sheet was obtained. The NR sheet was dried again in a vacuum oven at 70°C for one day and cut into small pieces before use.

3.2.1.2 PLA blends preparation

An internal mixer (Haake Rheomix 3000p) was employed to mix PLA pellets with dried NR, using a rotor speed of 50 rpm at 180°C for 20 minutes. The blend of both PLA blown film (4042D) and injection grade (3051D)

were prepared using the same condition. Further, the mixture was prepared using rotor speed of 40, 70 and 100 rpm when investigating effect of rotor speeds. PLA blend compositions at 0, 1, 3, 5, 10, 15 and 20 wt% rubber contents were prepared. Dried rubber and PLA pellets were dried in an oven at 70°C around eight hours to remove humidity in material before mixing. After exiting the chamber of the internal mixer, the mixture was cooled at room temperature for 30 minutes before being granulated by a grinder machine (Retsch grinder machine). All granulated mixtures were stored at room temperature for 24 hours before compression molded.

For mechanical testing, specimens of PLA mixtures were prepared by compression molding (Gotech model GT-7014-A30). Stainless steel mold was used. Geometry of the samples was given in each test below. The PLA mixtures were placed on the Teflon sheets, sandwiched between two flat metal plates. Each mixture was preheated at 180°C for 10 minutes and pumped five times before compressed at 180°C for 10 minutes. Then, the pressed sample was cooled at room temperature for 30 minutes before pushed out from the mold.

Dimension of the mold is varied. The rectangular mold with 180 x 180 mm², the thickness of 4 mm and 1 mm were used. Tensile and impact test specimens were prepared using a mold with thickness of 4 mm. Minimum of five specimens were used. For dynamic mechanical analysis, specimens were prepared with a width, thickness and height of 6, 1 and 19 mm, respectively. The sample disks for rheological test were prepared into a thickness of 1 mm and a diameter of 25 mm.

3.2.2 Mechanical properties

3.2.2.1 Tensile testing

Standard tensile testing was examined following ASTM D638. Dumbbell shape was prepared following type V, the thickness of 4 mm, the overall width of 9.53 mm, the overall length of 63.5 mm, the gage length of 7.62 mm and the gage width of 3.18 mm. Tensile testing was performed on 50 kN electronic load cell and mechanical grips using an Instron universal testing machine (model 5569). The test was conducted at a crosshead speed of 1 mm/min. All specimens were examined at room temperature. The data was acquired by a computer.

3.2.2.2 Impact testing

Notched Izod impact testing was examined following ASTM 256. Samples test were prepared by compression molding. The rectangular shaped specimen with the thickness of 4 mm, the width of 12.7 mm and the length of 64 mm was used. Notched Izod impact test was performed using an Atlas testing machine (model BPI). Before testing, all specimens were notched. The pendulum energy of 2.7J was used at room temperature. Minimum of five specimens were tested for each conditions.

3.2.2.3 Dynamic mechanical testing

Dynamic mechanical properties of PLA/NR blends were examined using dynamic mechanical analyzer (DMA) (Perkin Elmer model DMA 7e). Rectangular shape specimen with a width, thickness and height of 6, 1 and 19 mm, respectively was used. Measurement was performed with three-point bending mode between -100 to 80°C, with a constant strain of 0.02% at heating rate of 5°C/min, using liquid nitrogen as a cryogenic medium and controlled by the flow of

nitrogen gas of 20 ml/min. Constant frequency of 1 Hz was examined with dynamic controlling. Storage modulus (E') and tan delta ($\tan \delta$) were recorded as a function of temperature.

3.2.3 Rheological measurement

The rheological analysis was performed on a rheometer equipped with parallel-plate geometry (TA Instrument, AR-G2) under dynamic mode of shearing and a capillary rheometer (Kayeness). With the rheometer equipped with parallel-plate geometry, all measurements were performed at 180°C and angular frequency range of 0.1-100 rad/s. Disk-shape specimen with the thickness of 1 mm and diameter of 25 mm was used. The gap size was 1,000 μm and percent strain was 2. Complex viscosity (η^*) as a function of angular frequency were obtained. With the capillary rheometer, a capillary die with L/D of 15 and cone angle of 120° was used. A die length and diameter was 15.24 and 1.016 mm, respectively. The ground samples were used. All measurements were performed at 180°C in the shear rate range of 500-7,000 1/s. Shear viscosity (η) as a function of shear rate were determined.

3.2.4 Thermal properties

DSC (Perkin Elmer model DSC-7) analysis was used for determining thermal properties of the sample. The 5-10 mg samples were sealed in 40 μL aluminum pan. All samples were heated from 25 to 200°C at 10°C/min and kept isothermal for 2 min to erase previous thermal history. They were then cooled from 200 to 25°C at 10°C/min and heated to 200°C again at the rate of 10°C/min. Percentage of crystallinity of PLA in the blends was calculated by following equation (3.1). Enthalpy of fusion of PLA crystal is 93 J/g (Tsuji and Ikada, 1995).

$$X_c(\%) = \frac{\Delta H_{m,PLA} - \Delta H_{c,PLA}}{93 \times x_{PLA}} \times 100 \quad (3.1)$$

$\Delta H_{m,PLA}$: enthalpy of fusion of PLA (J/g)

$\Delta H_{c,PLA}$: enthalpy of crystallization of PLA (J/g)

x_{PLA} : weight fraction of PLA in blend

The glass transition temperature (T_g), cold crystallization temperature (T_{cc}), melting temperature (T_m) and degree of crystallinity (X_c) were determined from the second heat scanning. Both $\Delta H_{m,PLA}$ and $\Delta H_{c,PLA}$ were calculated using a software of DSC-7.

3.2.5 Morphology

Morphology of pure PLA and PLA/NR blends were characterized using scanning electron microscope (SEM) (JEOL model JSM-6400). Fracture surfaces from impact tested samples were coated with gold for 4-5 minutes prior to examination. Gold coating JFC-1100 electron microscope was used at an accelerating voltage of 10-20 kV. The particle size of NR was measured in representative zone of fractured impact specimens from SEM picture. Volume average particle size (\bar{d}_v) was calculated from a minimum of 200 particles following equation (3.2), where n_i is the number of particle and d_i is a diameter of particle (Grizzuti and Bifulco, 1997).

$$\bar{d}_v = \frac{\sum_i n_i d_i^4}{\sum_i n_i d_i^3} \quad (3.2)$$

Interparticle distance of NR particles was calculated using Wu's model following equation (3.3).

$$\tau = \bar{d}_w \left[\left(\frac{\pi}{6\phi} \right)^{1/3} - 1 \right] \quad (3.3)$$

τ is an interparticle distance, \bar{d}_w is a weight-average particle size and ϕ is a volume fraction of rubber. In this study, volume average NR particle size was used to calculate instead of weight average particle size.

CHAPTER IV

RESULTS AND DISCUSSION

In this chapter, the experimental results on PLA/NR blends were discussed. Specifically, effects of mixing temperature and rotor speed, rubber contents, and viscosity ratio on mechanical, thermal and morphological properties of blends were focused.

4.1 Effect of mixing temperature on physical properties and morphology of PLA blends

Mixing temperature is one significant factor affecting the morphology of the final polymer blends. As known, the blend morphology directly governs blend properties. Two mixing temperatures 180 and 200°C were examined. It is noted that during mixing the constant mixing force was obtained. This suggested that the steady state was attained.

4.1.1 Mechanical properties

The impact strength of the PLA/NR blends as a function of NR contents (wt%) was compared between two mixing temperatures, as shown in Figure 4.1. The impact strengths of PLA/NR blends mixed at 180°C are higher than that of 200°C for every compositions studied. As clearly seen, there is no difference in the strength of pure PLA at these two temperatures. Maximum impact strength was obtained at 10 wt% rubber for both mixing temperatures. This may be due to the higher viscosity of matrix phases at 180°C than at 200°C, as presented in Figure 4.2.

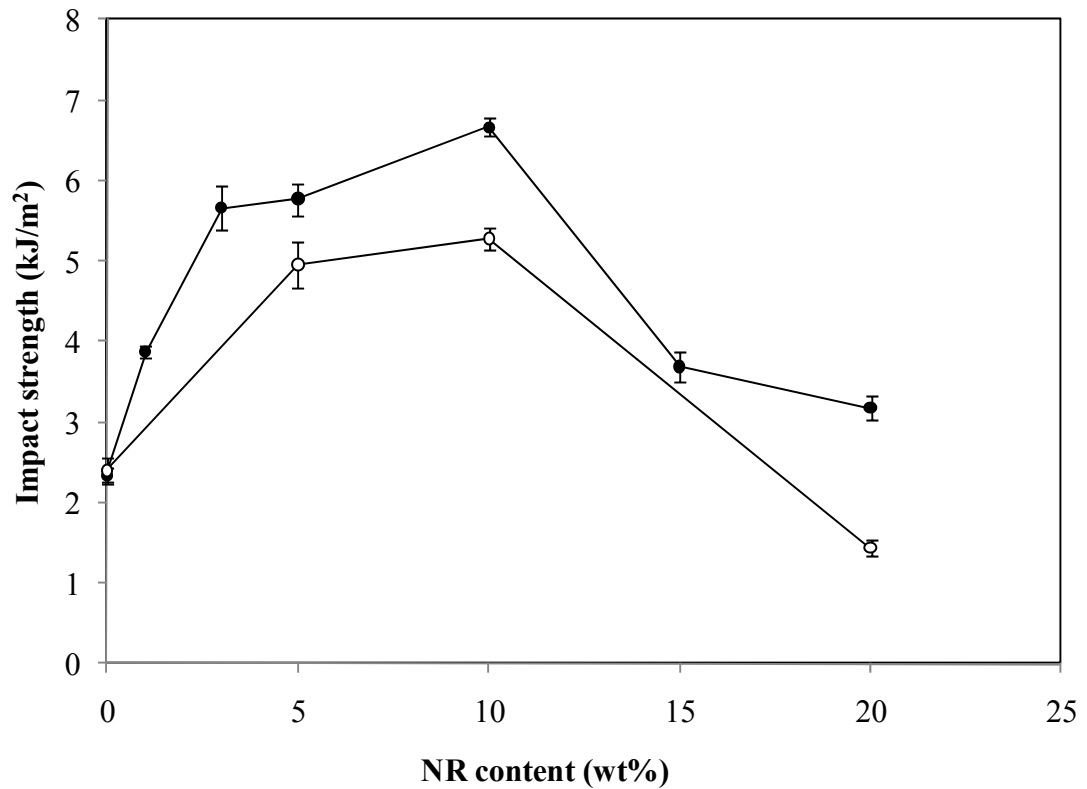


Figure 4.1 Impact strength of PLA blends with different NR contents at mixing temperature of (●)180 and (○) 200°C.

Tensile properties at mixing temperature of 200°C were investigated, tensile strength and percent elongation at break of PLA blends decreased with increasing NR content, as shown in Figure 4.3. The tensile strength and percent elongation at break were determined by reading the stress and extension at the point of specimen rupture, as indicated to the dash arrow line in Figure 4.3. Figure 4.4 shows tensile moduli and percent elongation at break as a function of NR contents when using a mixing temperature of 200°C. Young's moduli of the blends slightly decreased between 0-10 wt% NR content while percent elongation at break suddenly

decreased with increasing NR content. Young's modulus value was calculated from a slope of stress-strain curve between 0-2% strains.

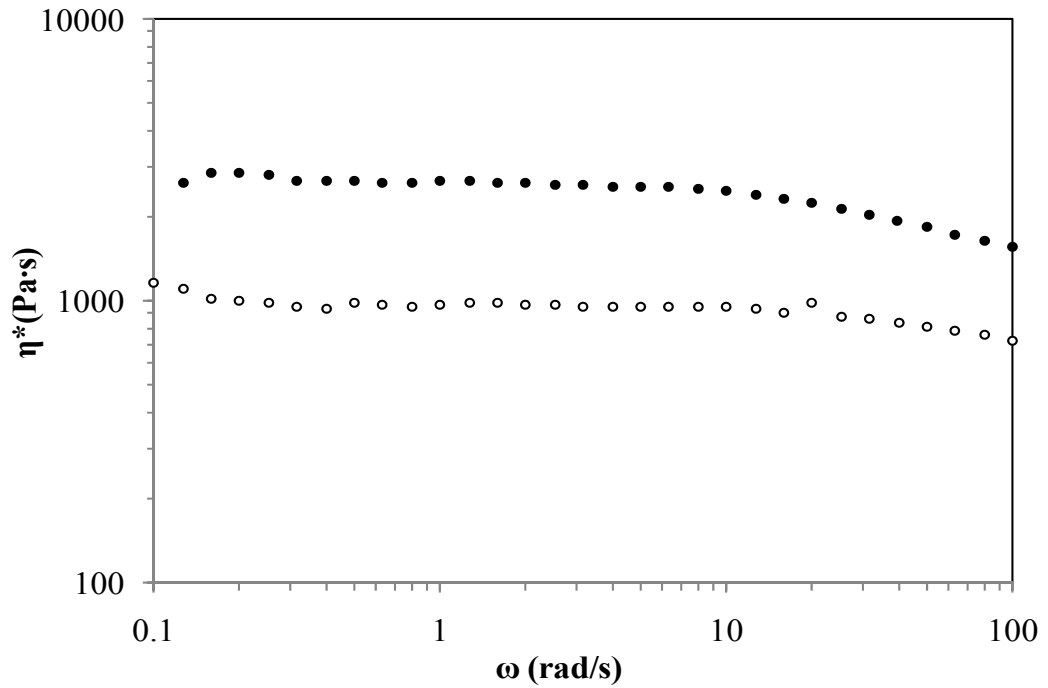


Figure 4.2 Complex viscosity of pure PLA at mixing temperature of 180°C (●) and 200°C (○) versus angular frequency.

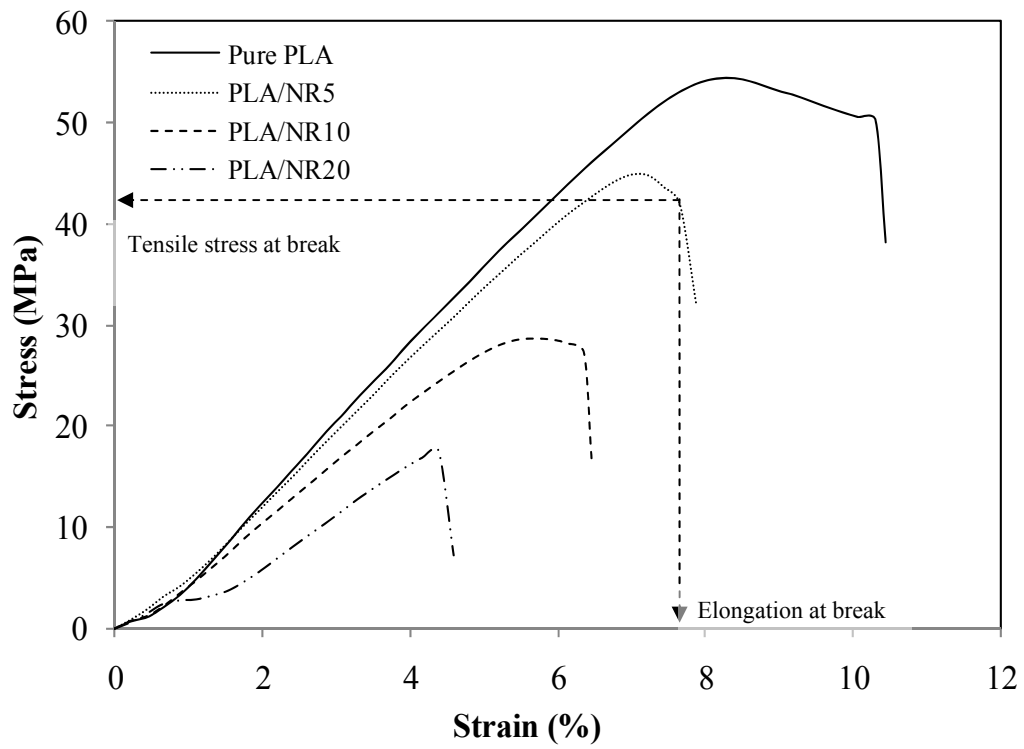


Figure 4.3 Tensile stress-strain curve of the PLA blends with different NR contents at mixing temperature of 200°C.

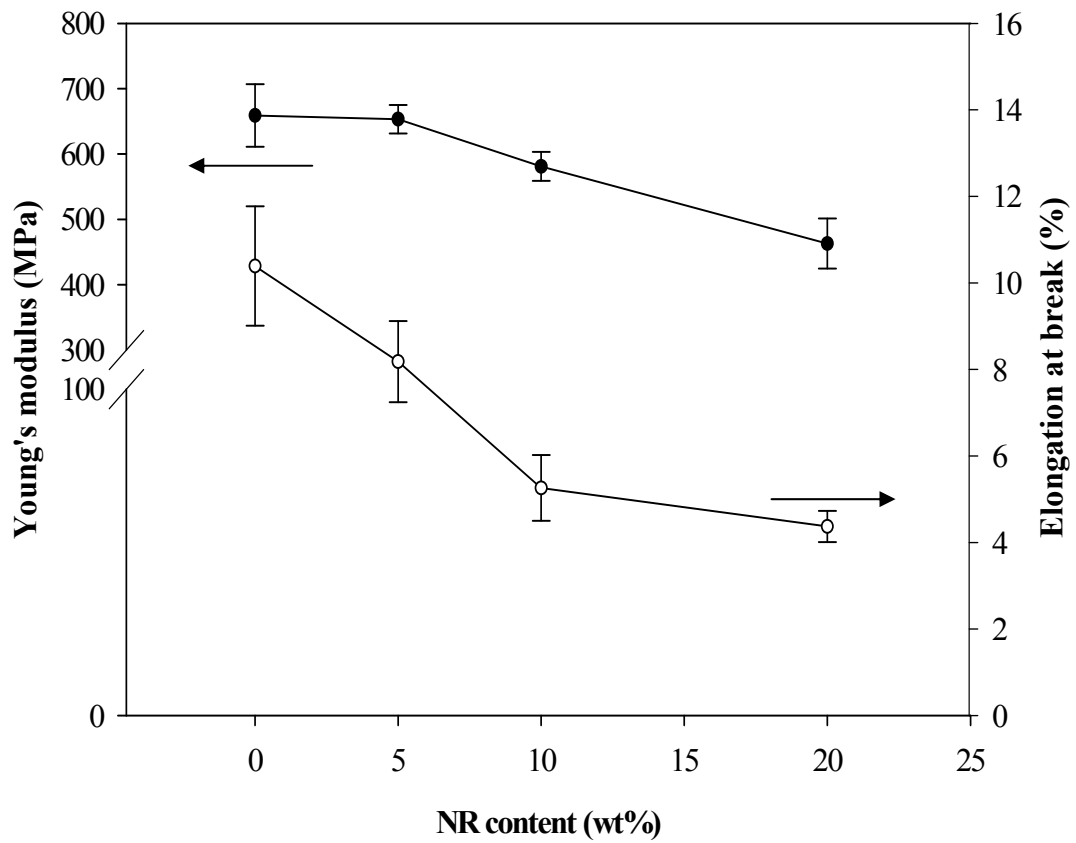


Figure 4.4 Mechanical properties of PLA blends as a function of NR contents: tensile moduli (●) and elongation at break (○).

Tensile properties with different NR contents at mixing temperature of 200°C were summarized in Table 4.1. Tensile toughness of the blends decreased with increasing NR contents as same as result of percent elongation at break. Toughness of pure PLA was 335.78 MPa. When adding NR content, toughness decreases to 40.38 MPa at 20 wt% NR. Toughness value was calculated from area under stress-strain curve.

Table 4.1 Tensile properties of pure PLA and PLA/NR blends at mixing temperature of 200°C.

NR content (wt%)	Modulus (MPa)	Tensile Strength (MPa)	Elongation at Break (%)	Toughness (MPa)
0	658.98	52.78	10.39	335.78
5	653.27	40.91	8.18	196.99
10	581.02	27.36	5.26	98.98
20	462.97	17.71	4.37	40.38

4.1.2 Morphology

SEM micrographs from impact fractured surface of PLA-5 wt% NR content with different mixing temperatures were presented in Figure 4.5. Spherical NR phases are evenly dispersed in continuous PLA matrix phase. This blend morphology shows that PLA and NR are immiscible. Lack of interaction and difference in solubility parameter between components could lead to thermodynamically immiscible PLA/NR blends. NR particle size was measured from SEM micrograph. The volume average NR particle size of the blends was calculated using equation (3.2). Volume average of NR particle sizes (\bar{d}_v) of 180°C and 200°C were 1.43 and 3.58 μm , respectively. These morphologies support the impact results. Smaller particle size typically promotes toughening more than larger size. The blends obtained at mixing temperature of 180°C exhibited smaller NR particle size and higher impact strength.

As mentioned in Chapter two, low viscosity ratio gives smaller droplet size. PLA matrix viscosity in Newtonian region (small shear rate) at 180°C is about three times higher than that of 200°C, as shown in Figure 4.2. Smaller NR particle

size obtained can be explained by the smaller viscosity ratio (η_{NR}/η_{PLA}) at mixing temperature of 180°C. Evenly dispersed of small NR particle size can dissipate applied energy better than large particle size.

These results revealed that PLA/NR blend at mixing temperature of 180°C yields higher mechanical properties than that of 200°C. Consequently, mixing temperature of 180°C was chosen for the rest of this study.

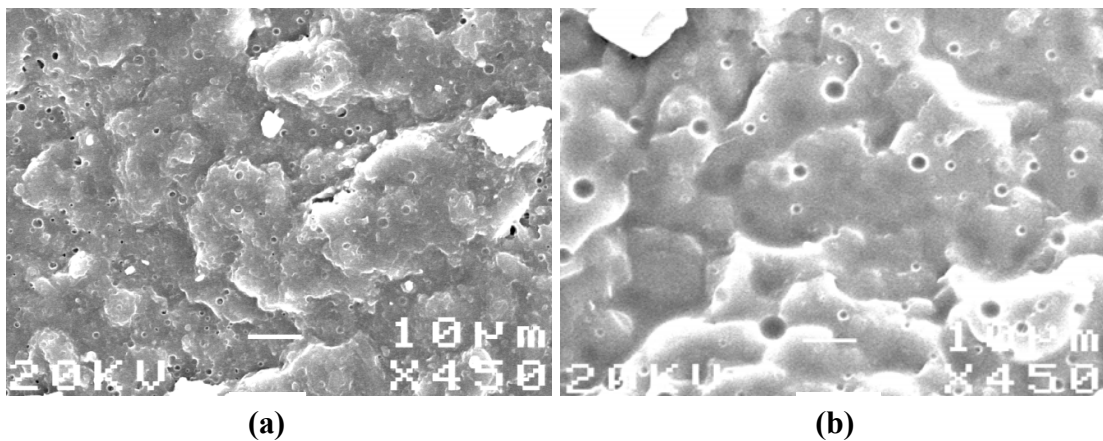


Figure 4.5 SEM micrographs of impact fractured surface of PLA-5 wt% of NR at mixing temperature of (a) 180°C and (b) 200°C.

4.2 Effect of rubber concentration and rubber particle size on physical properties of PLA blends

Increasing rubber concentration phase can decrease some properties of the blends such as modulus and tensile strength while toughness generally increases. In this section, NR concentration and NR particle size were investigated. The blends were prepared at the mixing temperature of 180°C.

4.2.1 Mechanical properties

Effect of natural rubber concentration between 0-20 wt% in PLA blend was investigated. Impact strength of pure PLA is 2.34 kJ/m². The impact strength increases with NR contents with the maximum of 6.66 kJ/m² at 10 wt%. More than 10 wt%, the strength significantly decreases as seen in Figure 4.1 (in the section 4.1.1). It is to mention that the impact strengths of the blends at 3, 5 and 10 wt% NR are not much different. Blend with 10 wt% NR content exhibits the highest impact strength.

Tensile stress-strain curves of pure PLA and PLA blends are shown in Figure 4.6. PLA shows the typical brittle behavior. All pure PLA specimens fracture without necking. Tensile strength and percent elongation at break of pure PLA are 57 MPa and 9.3%, respectively. Tensile strength of PLA blend tends to decrease with increasing NR content while elongation at break increases. The maximum elongation at break (up to 20.1%) is obtained when blending with 10 wt% NR. Yielding was observed at 5 and 10 wt% NR content. The appearance of tensile specimen after testing showed the stress whitening band perpendicular to tensile direction all over the gauge length. The yield was observed resulting in high percent elongation at break and area under tensile curve presented in Figure 4.6. Yielding can dissipate tension force that result in high toughness properties. Young's modulus and elongation at break of pure PLA and PLA blends determined from the stress-strain curves are depicted in Figure 4.7. Modulus of pure PLA was 634 MPa. Elongation at break increases with NR content up to 10 wt% then decreases. Only slightly decrease in Young's moduli was observed. This 10 wt% NR content also gave the maximum impact strength.

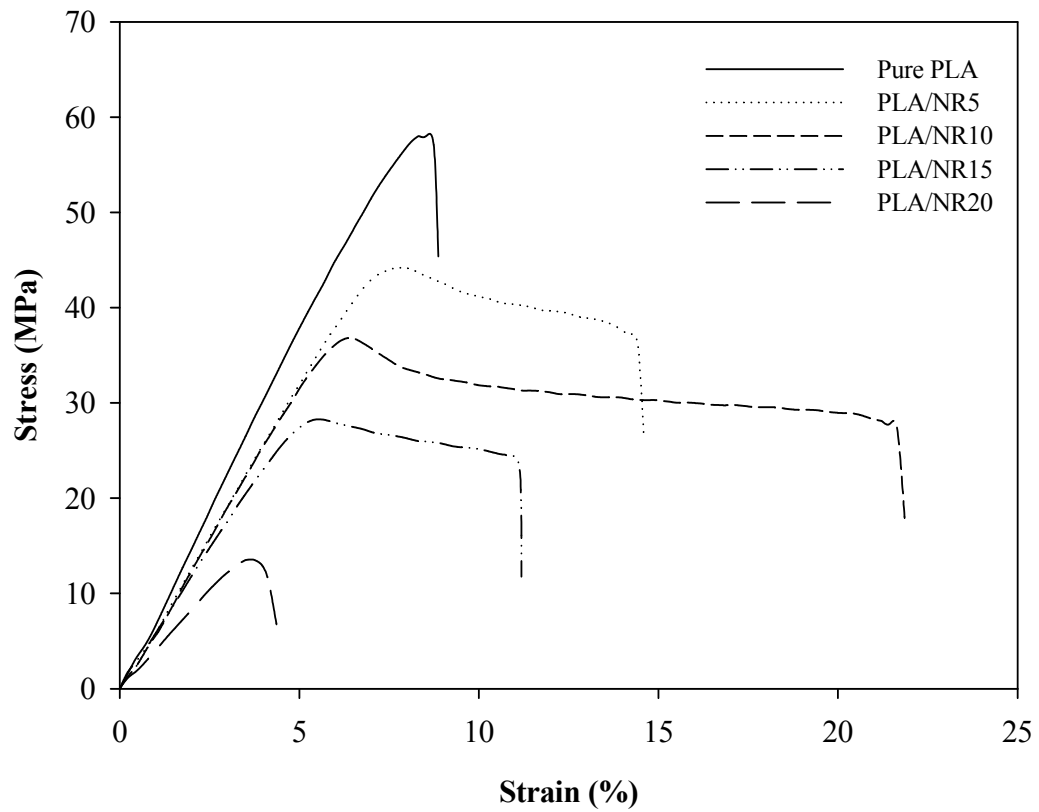


Figure 4.6 Tensile stress-strain curve of the PLA blends with different NR contents.

Tensile toughness of pure PLA and PLA blends were calculated from the area under stress-strain curve. The result exhibits toughness of PLA blends increased two folds compare to pure PLA. Tensile toughness of pure PLA was 317 MPa.

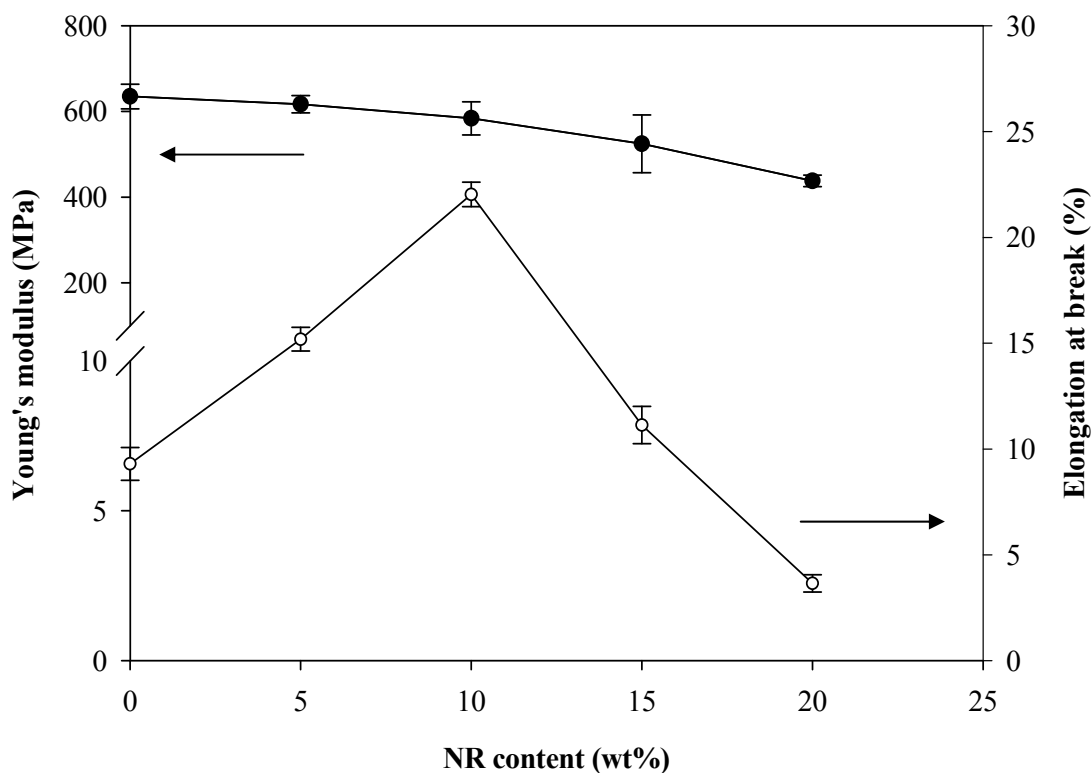


Figure 4.7 Mechanical properties of PLA blends as a function of NR contents: tensile moduli (●) and elongation at break (○).

Toughness increased up to 609 MPa at 10 wt% NR, as shown in Figure 4.8. Tensile toughness and percent elongation at break showed similar trend with impact results. As seen, the rubber content affects the blend properties. PLA blends containing 10 wt% NR exhibited highest toughness and impact strength.

4.2.2 Thermal properties

Thermal properties of pure PLA and PLA blends were investigated by DSC analysis. The glass transition temperature (T_g) is temperature that indicates the relaxation in polymer chain from glassy state to a rubbery state. Increasing temperature above T_g , molecular chain in amorphous region can rearrange to crystal form.

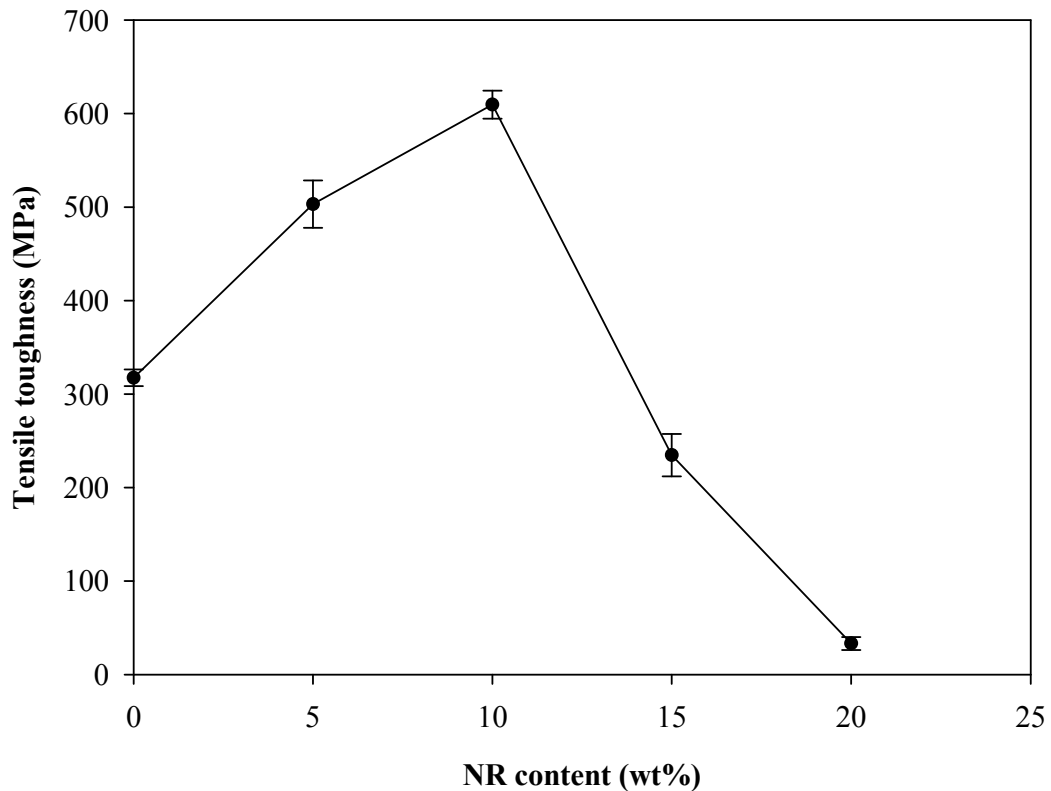


Figure 4.8 Tensile toughness of pure PLA and PLA blends with different NR contents.

Cold crystallization temperature is temperature where crystallization occurs under heating. T_{cc} is observed when heating over T_g but less than T_m . Melting temperature is observed when increasing temperature over than T_g and T_{cc} . T_m is a temperature that crystal of polymer melts. DSC second heating thermograms of pure PLA and PLA/NR blends are shown in Figure 4.9. For pure PLA (curve a), the glass transition temperature was found at 52.14°C. The exothermic peak at 116.06°C corresponds to the cold crystallization temperature appearing just before the endothermic melting peak. The double-peak melting temperature was observed. For pure PLA, the melting peak at lower temperature (T_{m1}) is higher than that at the

higher temperature (T_{m2}). Sarasua, Prud'homme, Wisniewski, Borgne, and Spassky (1998) studied and explained that the melting peak at higher temperature (T_{m2}) belongs to more perfect crystalline structure than that at lower temperature (T_{m1}). The less perfect crystals have enough time to melt and reorganize into crystals with higher structure perfection and remelt at higher temperature (Sarasua *et al.*, 1998). As shown in curve (b)-(e), the incorporation of NR did not affect the glass transition of PLA. No change in T_g suggests that there is no molecular interaction between PLA and NR. However, the T_{cc} was broadened when NR content increases.

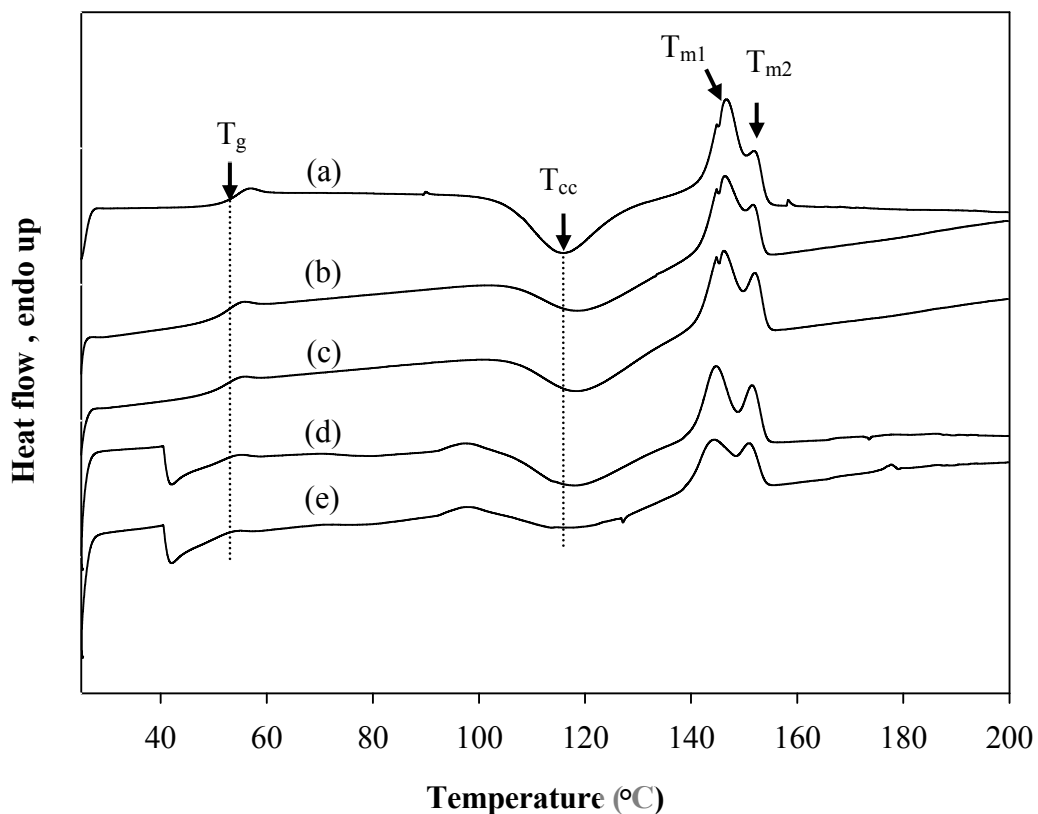


Figure 4.9 DSC thermograms of PLA/NR blends at heating rate of 10°C/min. Data from the second heat; (a) 0%NR, (b) 5%NR, (c) 10%NR, (d) 15%NR and (e) 20%NR.

In addition, the T_{m2} peak of the blends was clearly seen and became comparable to the T_{m1} peak as NR content increased. The presence of NR facilitates the crystallization process of PLA of higher degree of perfection. The data from the DSC second heating thermograms are summarized in Table 4.2. Degree of crystallinity (X_c) was calculated by equation (3.1), without the enthalpy of crystallization of PLA. NR content did not significantly affect the degree of crystallinity. These results suggested that the perfection of PLA crystalline structure can be induced by NR without interfering the crystallinity. Degree of crystallinity of PLA blends can be related to modulus of the blends. This result is similar to tensile modulus of the blends which slightly decreases or not significantly changes when adding NR content.

Table 4.2 Thermal properties of pure PLA and PLA blends with different NR contents (as obtained from DSC second heating thermograms).

NR content (wt%)	T_g (°C) DSC test	T_g (°C) DMA test	T_{cc} (°C)	T_m (°C)		X_c (%)
				T_{m1}	T_{m2}	
0	52.14	60.62	116.06	146.68	151.87	25.23
5	53.31	59.91	118.55	146.34	151.69	20.80
10	54.40	60.35	118.39	146.17	152.03	23.96
15	54.99	60.50	118.14	144.76	151.45	30.04
20	54.58	59.51	117.31	144.93	150.96	27.34

The DSC first heating thermograms of pure PLA and PLA/NR blends are shown in Figure 4.10. For pure PLA (curve a), T_g and T_{cc} were found at 55.11 and 118.07°C, respectively. Adding NR, T_g did not significantly change while T_{cc} slightly decreased, as summarized in Table 4.3. The double-peak melting temperature was not clearly observed. T_m of pure PLA was 147.35°C and did not significantly change when NR content increases. X_c was calculated by equation (3.1) and presented in Table 4.3. The % X_c obtained from the first heating thermograms does not significantly change with adding NR. DSC cooling thermograms of pure PLA and PLA/NR blends are shown in Figure 4.11. It clearly shows that no crystallization occurs under cooling at the rate of 10°C/min.

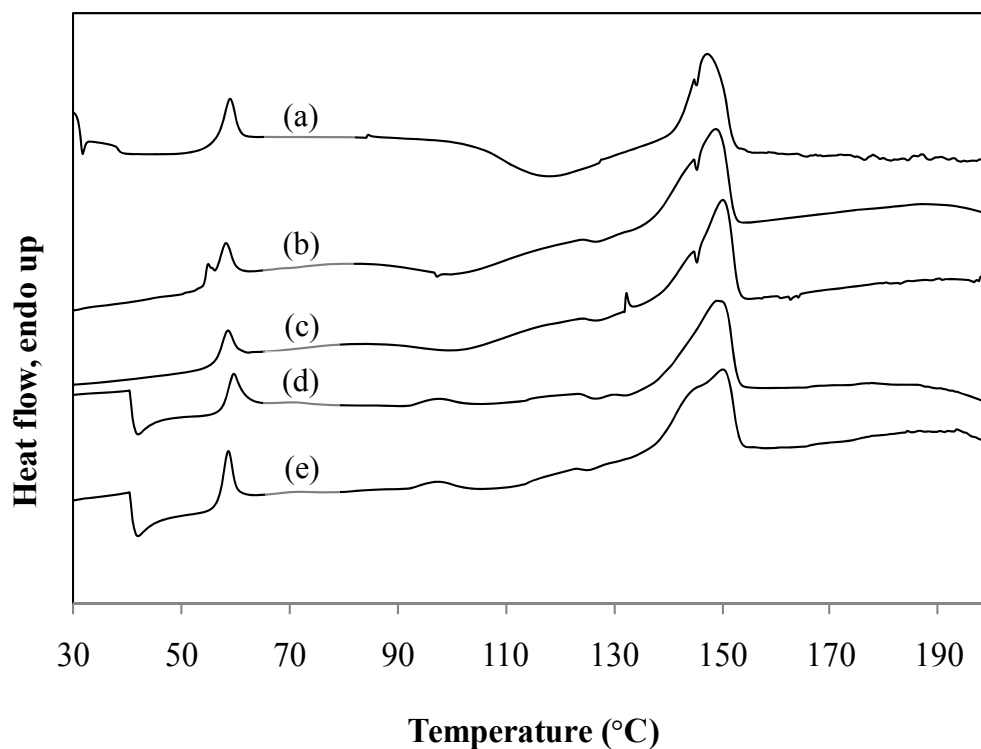


Figure 4.10 DSC thermograms of PLA/NR blends at heating rate of 10°C/min.

Data from the first heat; (a) 0%NR, (b) 5%NR, (c) 10%NR,
(d) 15%NR and (e) 20%NR.

Table 4.3 Thermal properties of pure PLA and PLA blends with different NR contents (as obtained from DSC first heating thermograms).

NR content (wt%)	T _g (°C)	T _{cc} (°C)	T _m (°C)	X _c (%)
0	55.11	118.07	147.35	41.07
5	54.24	100.00	148.68	39.23
10	56.00	101.97	150.02	39.10
15	57.44	107.10	149.13	36.50
20	56.42	108.44	150.12	42.99

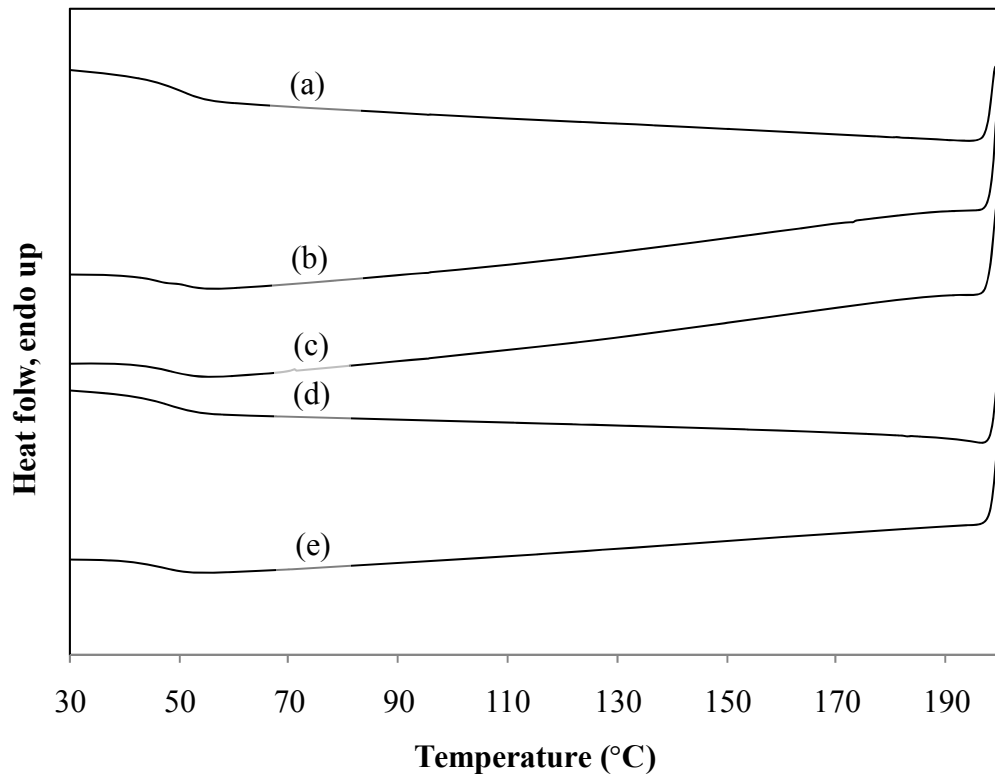


Figure 4.11 DSC thermograms of PLA/NR blends at cooling rate of 10°C/min:

(a) 0%NR, (b) 5%NR, (c) 10%NR, (d) 15%NR and (e) 20%NR.

4.2.3 Morphology

Mechanical properties result can be explained by phase morphology. Impact fractured surface of pure PLA and PLA blends were analyzed using SEM, as shown in Figure 4.12. Figure 4.12 (a) revealed the relatively smooth surface with small ridges of pure PLA, indicating the brittle fracture behavior. This smooth fractured surface agrees well with the small impact strength and elongation at break. Pure PLA is a brittle material. Fractured surface of PLA/NR blends became rough, as shown in Figure 4.12 (b-e). The blends show immiscible phases between NR and PLA matrix. The size of spherical NR phase became larger with the increase of NR content. It is also seen that voids are created as a result of drop of dispersed NR

phases. The rough fractured surface of PLA/NR blends indicates the ductile fracture behavior. Furthermore, impact fractured surface showed spherical rubber particles evenly dispersed in PLA matrix up to 10 wt% of NR content. This result indicates evenly dispersed of NR phases in PLA matrix influence impact strength of the blends up to optimum concentration. The average particle size of NR increased from 1.06 μm at 1 wt% NR to 2.3 at 10 wt% NR. NR particle size of 10 wt% around 2.3 μm is optimum size for PLA toughened. Figure 4.12 (f) and (g) exhibited large NR particles. This could be a result of coalescence of NR particles as particle-particle collides.

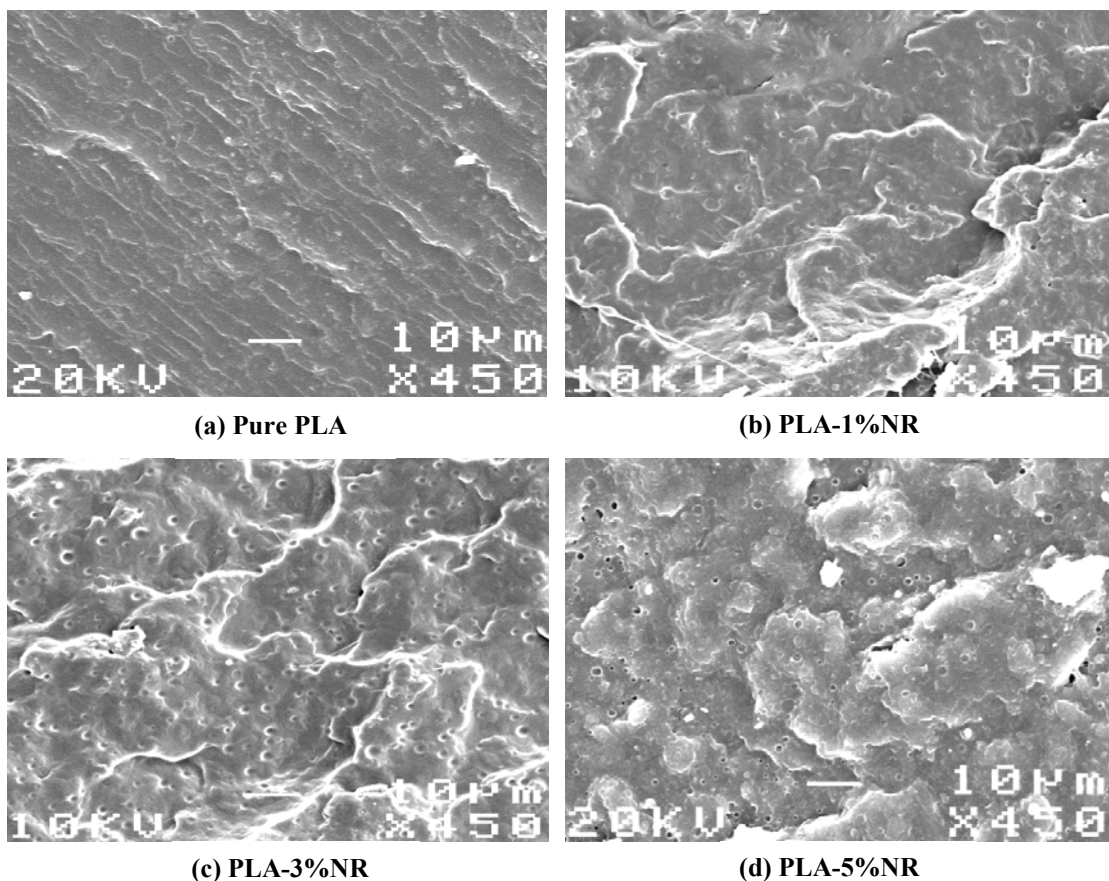


Figure 4.12 SEM micrograph of PLA/NR blends in the impact testing: (a) Pure PLA, (b) PLA-1%NR and (c) PLA-3%NR (— 10 μm).

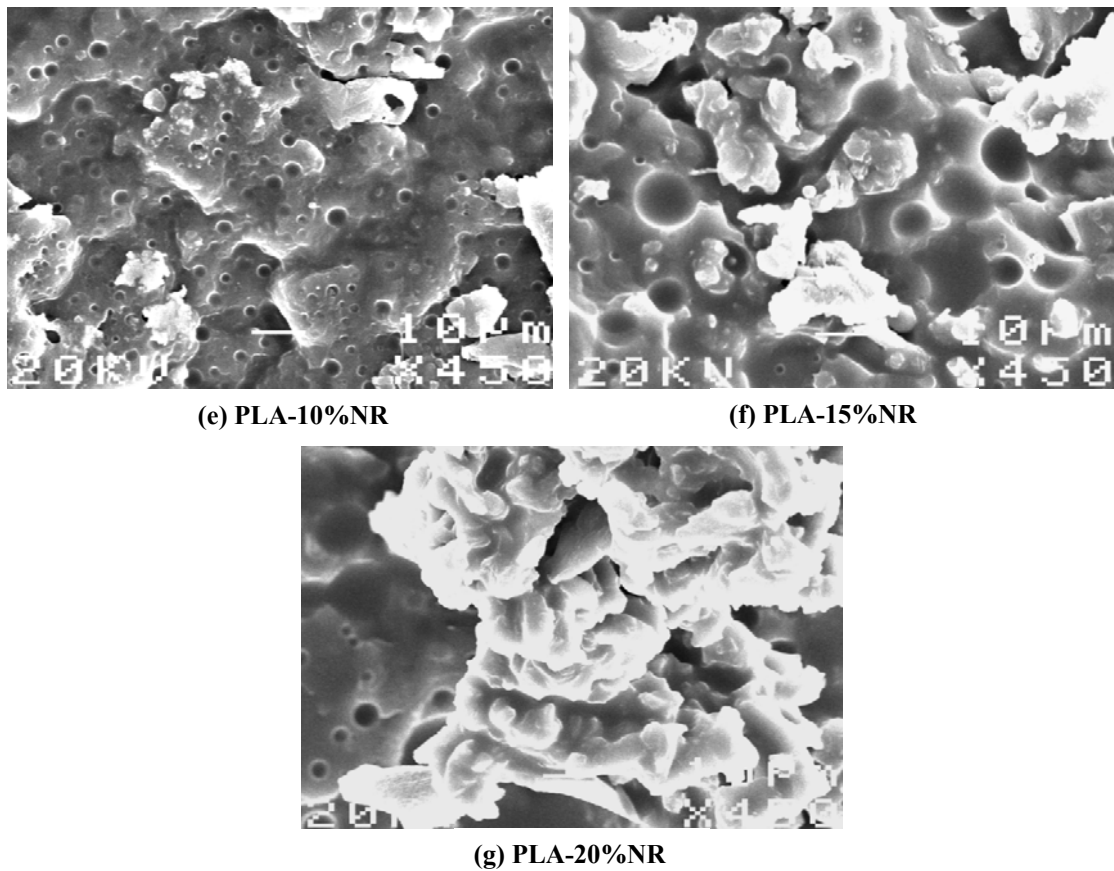


Figure 4.12 SEM micrograph of PLA/NR blends in the impact testing:

(d) PLA-5%NR, (e) PLA-10%NR, (f) PLA-15%NR and
(g) PLA-20%NR (— 10μm). (continued)

At 15 and 20 wt% NR contents, chances that NR particles collide are inevitably high. Drop of impact strength, elongation at break and tensile toughness at high rubber content suggests that the optimum NR content is required for toughening PLA. From SEM micrographs, NR particle size of the blends was determined using equation (3.2). The particle sizes of rubber were plotted as a function of rubber content, as shown in Figure 4.13. The average particle size gradually increases between 1-10 wt% of NR content. Then, the average particle size immediately

increased. Sundararaj and Macosko (1995) found that final particle size increases with the dispersed phase concentration due to increased coalescence. The particle size distribution also broadens at higher concentration. Noticeably, NR particle size did not significantly change between 1-10 wt% while impact strength increases as shown in Figure 4.1. Consequently, impact strength of the blends increases with increasing NR content in the range of 1-10 wt% NR. Adding NR content over than 10 wt%, particle sizes suddenly increase with increasing NR content. It can indicate that decreasing of impact strength at high NR concentration due to coalescence effect of NR particle.

As known, there is no clear separation between the role of the rubber content and rubber size on toughening. Consider that the NR sizes are similar (1.02-1.45 micron, shown in Figure 4.13) in the range of 1-5 wt% NR, the impact strengths were quite different. Among these contents, the 5 wt% NR gave the highest impact strength. Roughly, the results showed that the high rubber content offers more toughening at the same particle size.

As presented above, PLA blends containing 10 wt% of NR exhibits the highest impact strength and percent elongation at break. High toughness was produced from optimum of both NR content and particle size. In literature review, both content and particle size of rubber phase influence toughness of the blend, these parameters are related to interparticle distance (τ) of rubber phase. Wu proposed that τ is significant parameter that dominates the brittle to tough transition. Interparticle distance consists of weight average particle size and volume fraction of rubber as presented in equation (2.1) or (3.3). According to Wu's model, the tough polymer blends can be obtained if τ is smaller than critical interparticle distance (τ_c) (Wu,

1985). τ_c is defined from plotting the impact strength as a function of τ at which impact strength suddenly decrease. In this study, τ was determined using equation (2.1) or (3.3). Average by volume of NR particle size was used to calculate. Interparticle distance and impact strength with different NR contents are listed in Table 4.4.

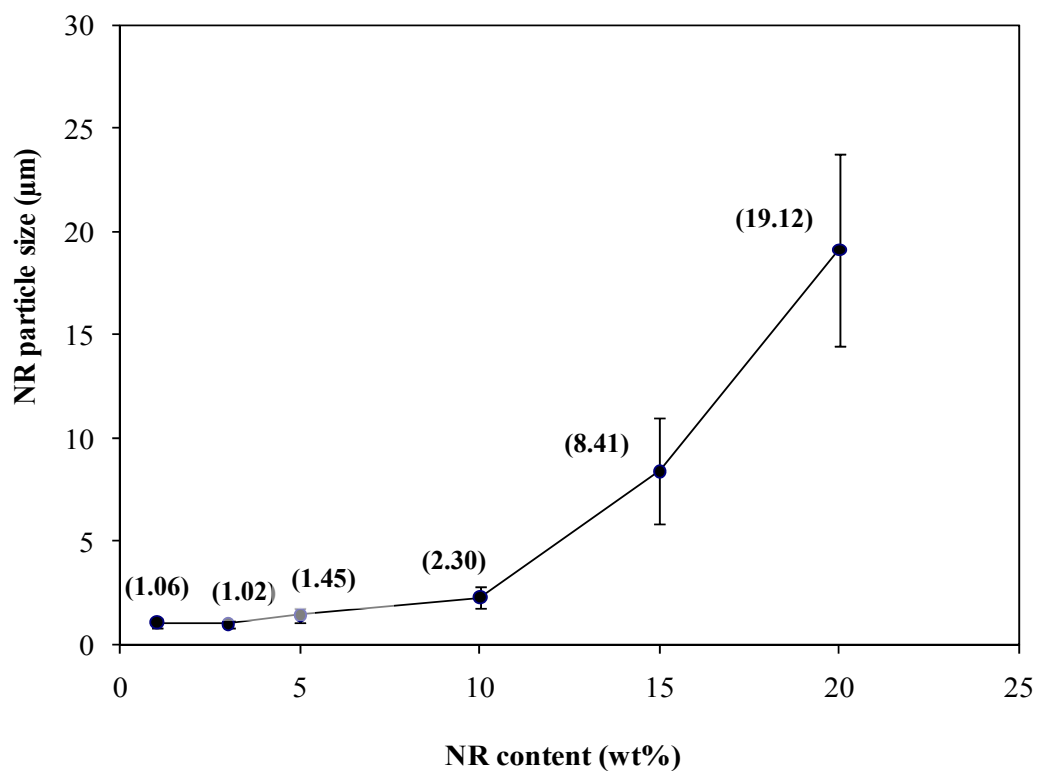


Figure 4.13 NR particle size (\bar{d}_v) in PLA/NR blends with NR contents.

In Table 4.4, it is clear that τ about 1.7 micron is optimal for impact toughness. When τ is more than 1.7 micron, the impact strengths decrease. At NR content of 10 wt%, the maximum impact strength was obtained at which τ is about 1.7 micron and the NR particle size is 2.3 micron.

4.2.4 Dynamic mechanical properties of PLA blends

Dynamic mechanical analysis (DMA) measures stiffness and damping, reported as modulus and tan delta ($\tan \delta$). Storage modulus is the measure of the elastic part in material. The ratio of the loss to the storage is the $\tan \delta$. In this study, storage modulus (E') and $\tan \delta$ of pure PLA and PLA/NR blends as a function of temperature are shown in Figure 4.14 and 4.15.

Table 4.4 Interparticle distance (τ) and impact strength with different NR contents.

NR content (wt%)	Interparticle distance (μm)	Impact strength (kJ/m^2)
1	2.90	3.87
3	1.62	5.66
5	1.72	5.77
10	1.69	6.66
15	4.34	3.69
20	7.22	3.18

In storage modulus curve, a glass transition of pure PLA was around 55 to 60°C. A glass transition region of NR exhibited around -90 to -80°C. The result exhibited that a glass transition region of PLA in the blends did not change with adding NR. Besides, there was no change in storage modulus in glassy state with increasing NR content, as shown in Figure 4.14. Increasing of storage modulus after glass transition range around 70°C may be due to the increase in PLA chains mobility. Some chains are possibly twisted and interlaced with each other. Martin and Avérous

(2001) expected the increase of chain mobility supported the crystallization process, above T_g .

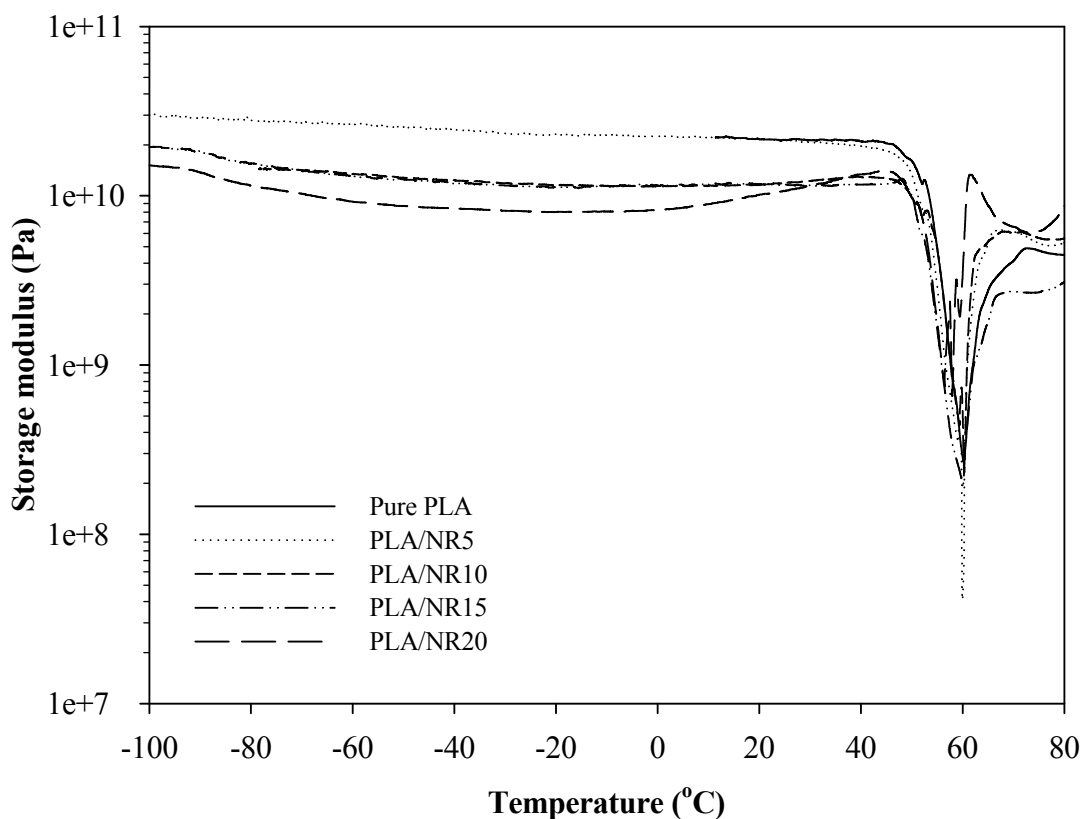


Figure 4.14 Storage modulus curve of pure PLA and PLA/NR blends with different NR contents.

Tan δ or damping is a measure of energy dissipation and indicates capability of absorbing energy. Tan delta peak of pure PLA shows around 60°C (peak maximum), corresponding to the glass transition temperature, as shown in Figure 4.15. Glass transition temperature of PLA in the blends did not significantly change with adding NR, as presented in Table 4.2. This indicates the lack of significant molecular interaction between PLA and NR phases. Tan delta peak of pure PLA is

broad while PLA/NR blends of 5 and 10 wt% NR content exhibited sharp peak and high intensity. This result suggested that the blends with 5 and 10 wt% NR contents can dissipate energy more than that of pure PLA. The height of $\tan \delta$ peak relates to the damping ability. The higher the height the more the dissipated energy. The high energy dissipation can be related to impact strength of PLA blends with 5 and 10 wt% NR. Both contents show high impact values. Adding NR more than 10 wt%, $\tan \delta$ peak showed low intensity peak. As discussed earlier, the coalescence of NR particles occurs that influences dissipation energy of the blends.

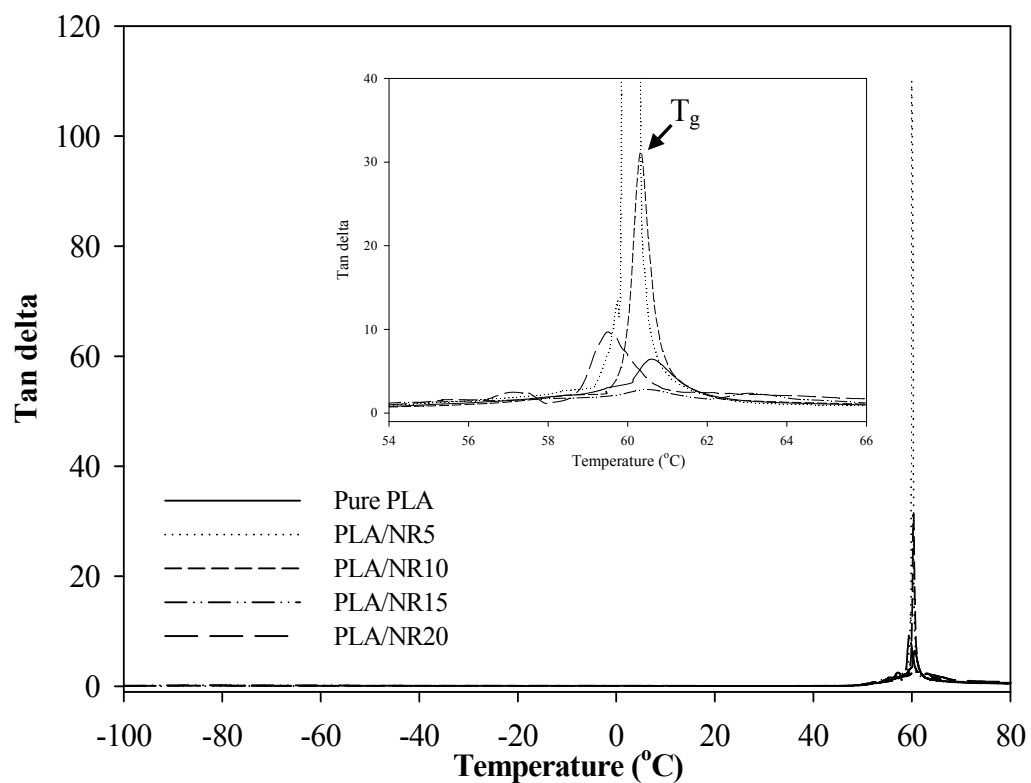


Figure 4.15 Tan delta curve of pure PLA and PLA/NR blends with different NR contents.

Therefore, adding NR content between 5-10 wt% provides high toughness due to the ability to absorb high applied energy.

4.3 Effect of rotor speeds on physical properties of PLA blends

In section 4.2, NR content, NR particle size and interparticle distance influence toughness improvement of PLA blends. In this section, effect of rotor speeds on NR particle size was investigated, rotor speeds of an internal mixer was related to shear rate of system.

Droplet deformation and breakup influence morphology and mechanical properties of polymer blends. Taylor design equation which is the ratio of viscous stress to interfacial stress. This ratio is Capillary number (Ca), as shown in equation (2.2). PLA-5 wt% and PLA-10 wt% NR with different rotor speeds were investigated. Difference in rotor speed should affect droplet deformation and breakup of NR phase. As known, at small shear rate the viscosity is constant (Newtonian region) and at high shear rate the viscosity decreases (shear-thinning region). With varying rotor speeds in an internal mixer, the matrix viscosity (η_m) could either be constant or decrease. If η_m does not change in Newtonian region when increasing shear rate, increasing of shear rate would result in high viscous stress ($\eta_m \dot{\gamma}$) and Ca number. In shear thinning region, η_m will decrease when increasing shear rate. Therefore, increasing of shear rate might not affect in viscous stress and Ca number. If shear rate is in Newtonian region, viscous stress will be increased and Ca becomes more than Ca_{crit} . Therefore, droplet can deform to long filament (small radius of droplet) and breakup. Assuming

that interfacial stress does not change with shear rate, small droplet size would then be obtained.

4.3.1 Mechanical properties

By varying the rotor speeds (40, 50, 70, and 100 rpm), impact strength of the blends at 5 and 10 wt% of NR was studied. As shown in Figures 4.16 and 4.17, both contents exhibit relatively the same impact strength regardless of rotor speed (as guided line). In addition, it can be seen that both 5 and 10 wt% NR content exhibited impact strength around 6 kJ/m².

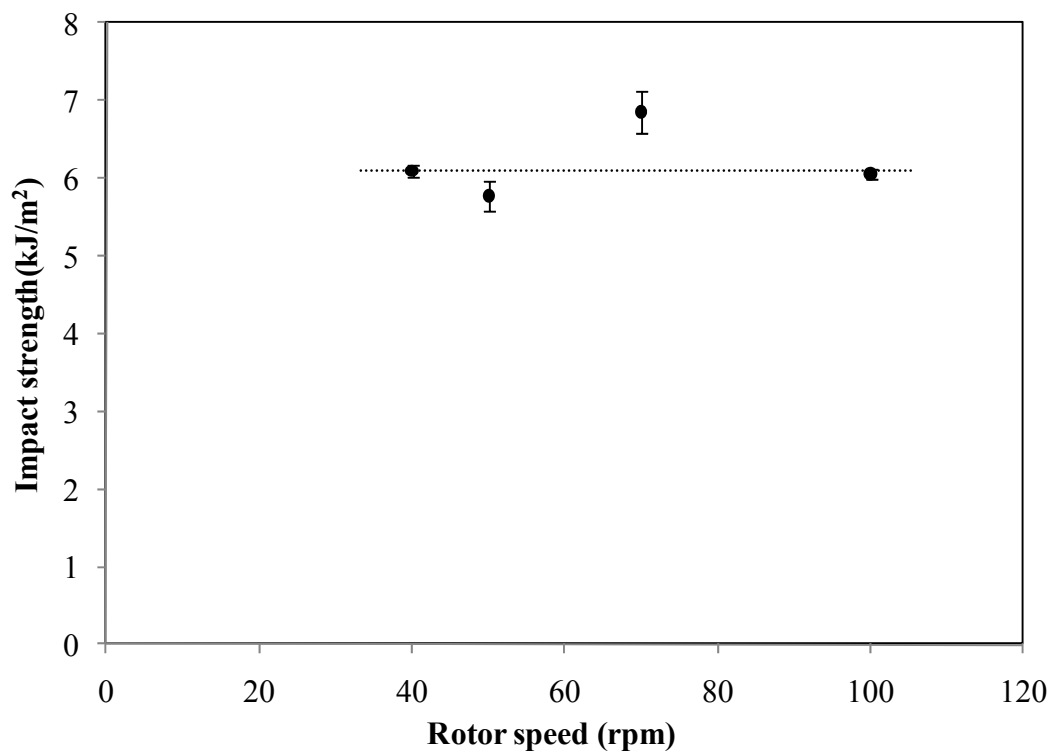


Figure 4.16 Impact strength of PLA-5%NR content with different rotor speeds.

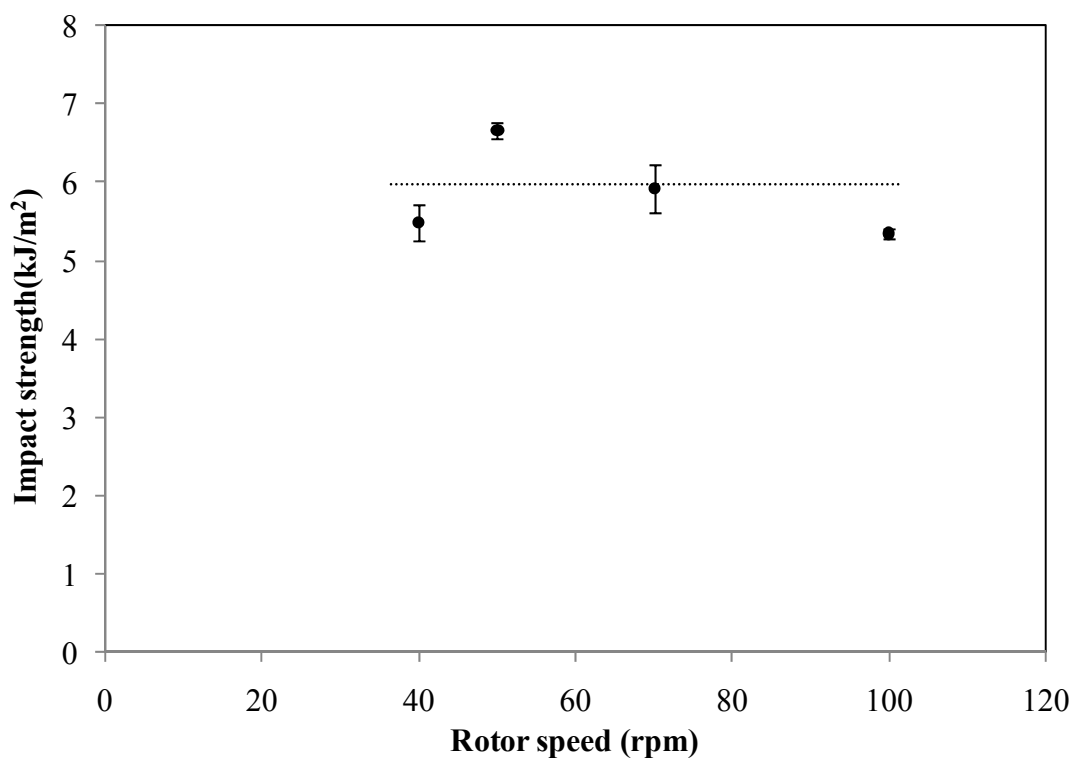


Figure 4.17 Impact strength of PLA-10%NR content with different rotor speeds.

4.3.2 Morphology

SEM micrographs from impact fractured surfaces of 5 and 10 wt% NR contents with various rotor speeds are shown in Figure 4.18 and 4.19. All fracture surfaces showed rough fracture surface with rubber particles evenly dispersed in PLA matrix. Average particle size of NR phase was measured. NR particle size did not significantly change as summarized in Table 4.5. This result suggests that rotor speeds used in an internal mixer generated small shear rate range (Newtonian region), not enough to change viscous stress.

According to capillary number, matrix viscosity is a function of shear rate, as shown in equation (4.1).

$$Ca = \frac{\eta_m(\dot{\gamma})\dot{\gamma}R}{\Gamma} \quad (4.1)$$

Following equation (4.1), when viscous stress and interfacial tension did not change, capillary number does not change. When capillary number with different rotor speeds did not significantly change, it resulted in no change of droplet deformations of rubber phase. When interfacial tension is dominated, NR particle size did not change. This result can be concluded that the rotor speeds between 40 and 100 rpm are small rate, therefore, they did not affect NR particle size of the blends.

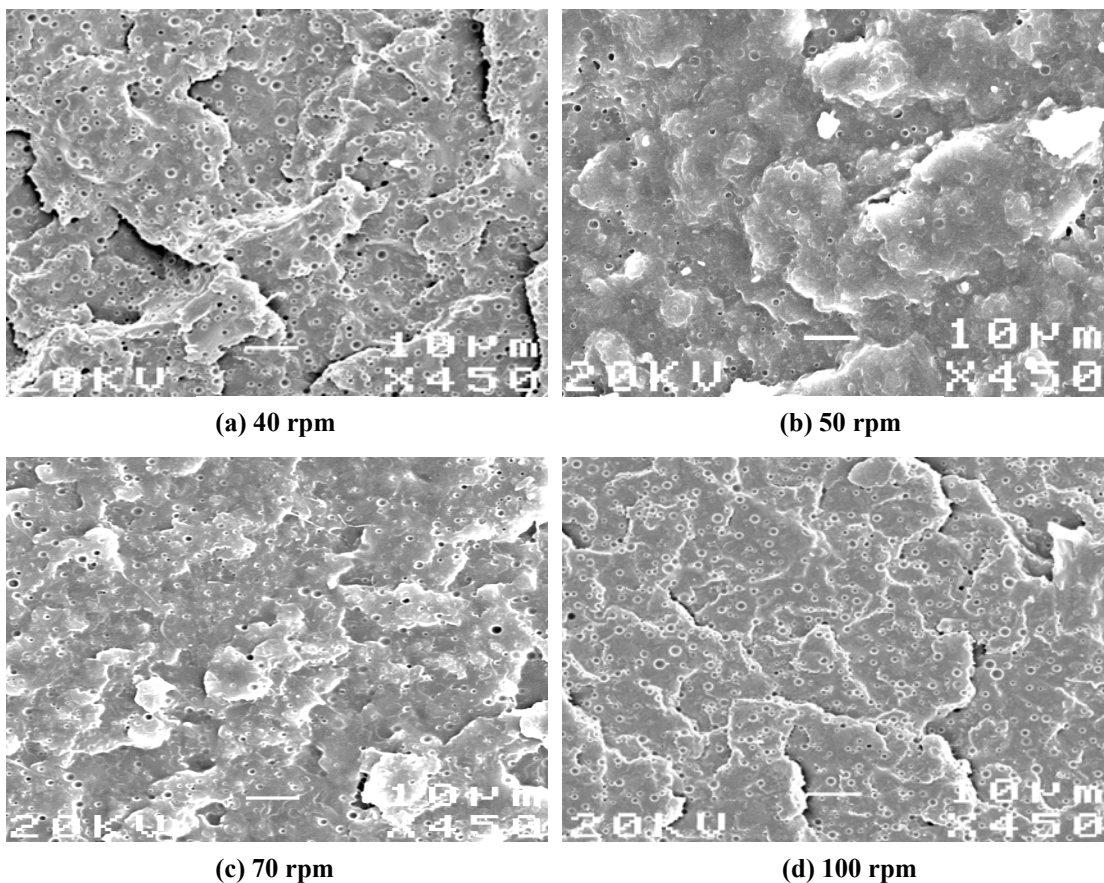


Figure 4.18 SEM micrograph of PLA-5%NR content with various rotor speeds:

(a) 40 rpm, (b) 50 rpm, (c) 70 rpm and (d) 100 rpm (— 10 µm).

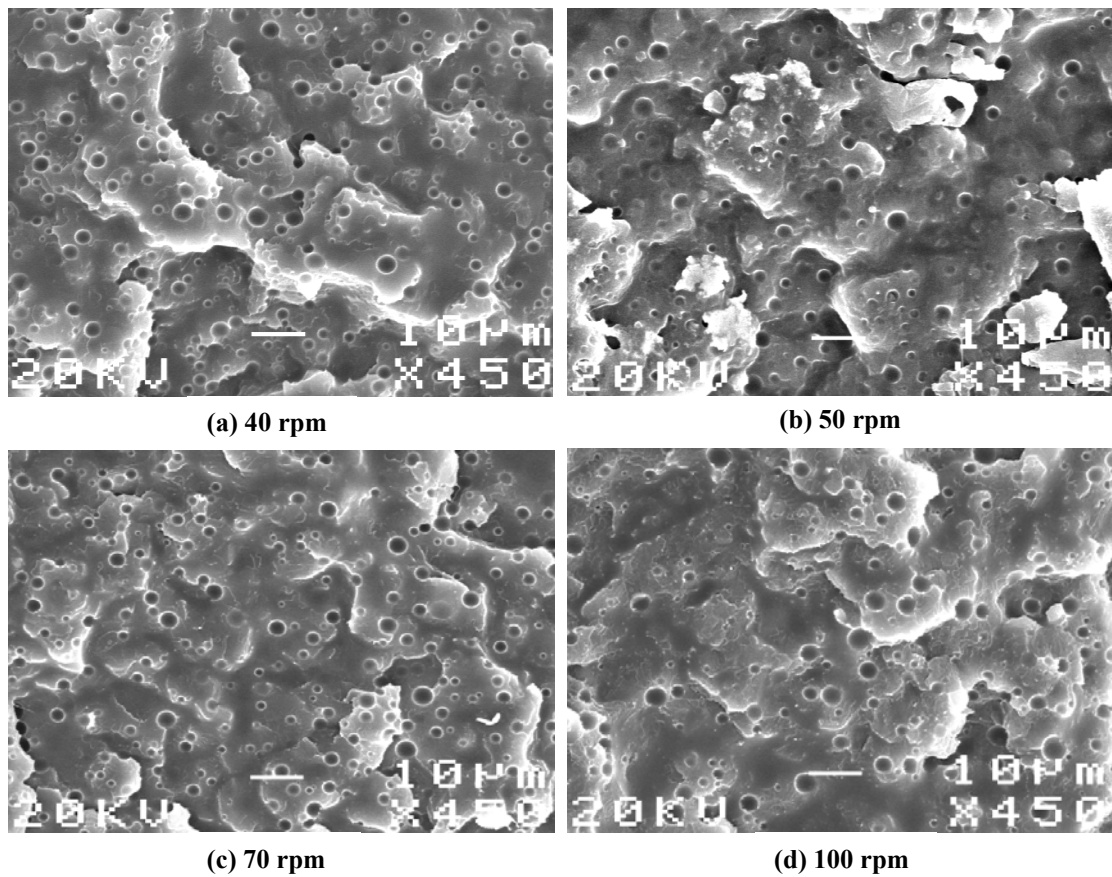


Figure 4.19 SEM micrograph of PLA-10%NR content with different rotor speeds:

(a) 40 rpm, (b) 50 rpm, (c) 70 rpm and (d) 100 rpm (— 10 µm).

Table 4.5 NR particle sizes with various rotor speeds PLA-5% and PLA-10%NR contents.

Rotor speeds (rpm)	NR particle sizes (µm)	
	5 wt%NR content	10 wt%NR content
40	1.15 ± 0.30	2.42 ± 0.67
50	1.43 ± 0.39	2.30 ± 0.79
70	1.60 ± 0.43	2.65 ± 0.67
100	1.35 ± 0.36	2.82 ± 0.87

Impact strength result at various rotor speeds can be related with impact strength result at various NR contents as shown in Figure 4.1. Impact strength of both 5 and 10 wt% NR with various rotor speeds is in the range of 5 to 7 kJ/m². This impact range is similar to that of 3, 5 and 10 wt% NR. From impact strength results, it can be concluded that impact strength in the range of 5 to 7 kJ/m² may be the maximum range of PLA/NR blends. Adding 10 wt% of NR content gave maximum impact strength. Therefore, NR particle size in PLA blends with 10 wt% NR is an optimum particle size (2.3 μm) that gives the highest impact toughness.

4.4 Effect of viscosity ratio on physical properties of PLA blends

One factor influencing on droplet deformation and breakup of disperse phase is viscosity ratio between two phases. Therefore, effect of viscosity ratio on mechanical properties and morphology of PLA/NR blend was investigated in this section.

4.4.1 Mechanical properties

According to Taylor theory, PLA matrix grade was varied to study the effect of viscosity ratio on NR particle size. Effect of viscosity ratio (η_{NR}/η_{PLA}) was investigated using PLA matrix blown film grade (4042D) compared to injection grade (3051D). Both grades were mixed with 10 wt% NR by a rotor speed of 50 rpm. Impact strength value of PLA blend at 10 wt% NR content using PLA matrix blown film grade and injection grade are 6.66 and 5.33 kJ/m², respectively. From the section 4.3, rotor speeds in an internal mixer of 50 rpm is in a Newtonian region. This result suggests PLA matrix viscosity is constant as a function of shear rate. Viscosities of two PLA grades are shown in Figure 4.20. Complex viscosity of PLA blown film

grade is higher than that of injection grade. The viscosity of PLA blown film and injection grade with different shear rate were investigated by two methods. At small rate, two PLA grades were examined using small amplitude oscillatory shear (SAOS) rheometer analysis while at high rate using capillary rheometer analysis.

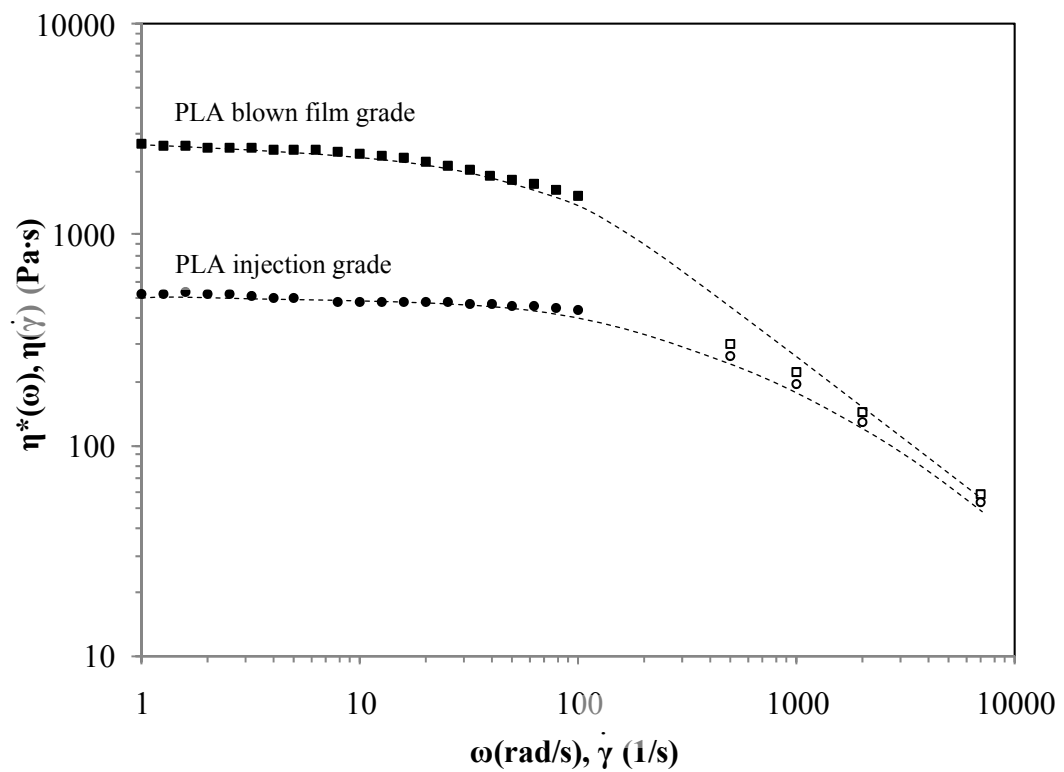


Figure 4.20 Plot of shear viscosity, $\eta(\dot{\gamma})$ and complex viscosity, $\eta^*(\omega)$ of PLA

blown film grade (\square) and injection grade (\circ) versus shear rate ($\dot{\gamma}$) and angular frequency (ω). The $\eta^*(\omega)$ data (closed symbol) were determined using SAOS with a parallel plate rheometer; the $\eta(\dot{\gamma})$ data (opened symbol) were obtained with a capillary rheometer.

4.4.2 Morphology

From Taylor's theory, viscosity ratio is a factor influence droplet deformation and breakup. Viscosity ratio relates with a critical capillary number following equation (2.3). In this section, PLA/NR blends using small shear rate in an internal mixer of 50 rpm. PLA/NR blends using PLA blown film grade has lower viscosity ratio than that of injection grade since it has higher matrix viscosity, as shown in Figure 4.20. The lower viscosity ratio of the blends produced smaller particle sizes and higher impact strength than that high viscosity ratio.

SEM micrographs of PLA blends at 10 wt% NR content with different PLA matrix grade were shown in Figure 4.21. Impact fractured surface of the blends with PLA matrix blown film grade (lower viscosity ratio) shows smaller NR particle size compared to PLA matrix injection grade (high viscosity ratio). NR particle sizes of the blends with PLA matrix blown film grade and injection grade are 2.30 ± 0.97 and 3.9 ± 1.67 μm , respectively. Small NR particle size of the blends with PLA matrix blown film grade due to smaller viscosity ratio affect critical capillary number, as shown in equation (2.2). Critical capillary number decrease with viscosity ratio decrease up to η_r around one. Grace proposed that droplet can be broken up when $\eta_r < 4$, as shown in Figure 2.4 (in Chapter two). At low rate, the viscosity of PLA blown film grade is higher than that of injection grade, as shown in Figure 4.20. Therefore, droplet of NR in PLA blends with PLA matrix blown film grade can be deformed to long filament (smaller radius of droplet) and breakup to smaller particle size easily than PLA matrix injection grade. From discussed above, this result indicated that effect of viscosity ratio influence NR particle size.

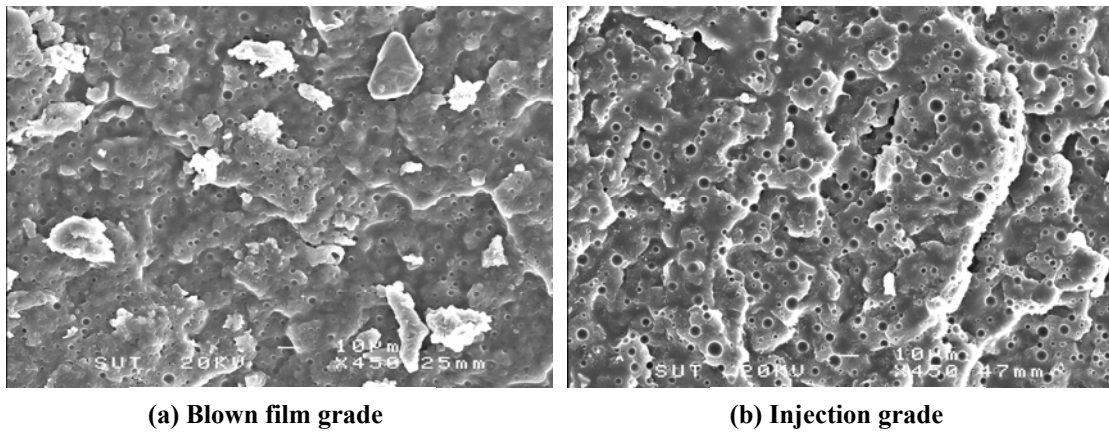


Figure 4.21 SEM micrograph of PLA/NR10 with different PLA matrix grade:

(a) blown film grade and (b) injection grade (— 10 μm).

CHAPTER V

CONCLUSIONS

Toughness of PLA was improved by blending with NR. Both NR content and NR particle size in PLA blends influence toughness properties. Adding NR of 10 wt% gave the highest impact strength. Toughness of the blends increases two folds compared to pure PLA. Average NR particle size of PLA-10 wt% NR content is 2.30 μm and it is an optimum size to toughness improvement. Mixing temperature of 180°C was used to prepare PLA and NR blend due to it produces high impact strength and small NR particle size. Rotor speeds of an internal mixer between 40 to 100 rpm did not significantly change impact strength and NR particle size of the blends. At 5 and 10 wt% of NR contents, impact strength with various rotor speeds was a similar range between 5 to 7 kJ/m^2 . This result relates with impact strength at various NR contents between 3 to 10 wt%. Therefore, an optimum NR particle size which produced highest impact toughness is 2.30 μm . The viscosity ratio, η_r influences impact strength and NR particle size by which lower η_r shows higher impact strength and smaller NR particle size. This result supports effect of optimum size on toughness improvement. Storage modulus from DMA testing did not significantly change with adding NR. Height of $\tan \delta$ peak at 5 and 10 wt% NR reveals that the blends can dissipate high energy therefore toughness are improved. Two peaks of $\tan \delta$ exhibited immiscibility of the blends. The presence of NR phase in PLA matrix did not change T_g , T_{cc} and T_m of PLA in the blends. Percent of crystallinity did not change with

adding NR phase while perfection of PLA crystalline structure was induced by NR.

Crystallinity of the blends did not influence toughness of PLA blends.

REFERENCES

- Arostegui, A., Gaztelumendi, M., and Nazabal, J. (2001). Toughened poly(butylene terephthalate) by blending with a metallocenic poly(ethylene-octene) copolymer. **Polymer**. 42: 9565-9574.
- Bhatia, A., Gupta, R. K., Bhattacharya, S. N., and Choi, H. J. (2007). Compatibility of biodegradable poly (lactic acid) (PLA) and poly (butylene succinate)(PBS) blends for packaging application. **Korea-Australia Rheology Journal**. 19.
- Blackley, D.C. (1987). **In Encyclopedia of Polymer Science and Engineer**, 2nd.
- Cho, K., Yang, J., and Park, C.E. (1998). The effect of rubber particle size on toughening behavior of rubber-modified poly(methyl metacrylate) with different test methods. **Polymer**. 39: 3073-3081.
- Einstein, A. (1906). **Ann. Physic**. 19: 289.
- Flexman, E.A. (1993). **Toughened plastics I; science and engineering**. P. 79-80.
- Grace, HP. (1982). Dispersion phenomena in high viscosity immiscible fluid systems and application of static mixers as dispersion devices in such systems. **Chem. Eng. Commun**. 14: 225-77.
- Guerrica-Echevarfa, G., Eguiazabal, J. I., and Nazabal, J. (2007). Influence of compatibilization on the mechanical behavior of poly(trimethylene terephthalate)/poly(ethylene-octene) blends. **Eur Polymer J**. 43: 1027-1037.
- Grizzuti, N. and Bifulco, O. (1997). Effects of coalescence and breakup on the steady-state morphology of an immiscible polymer blend in shear flow. **Rheol Acta**. 57: 406-415.

- Huang, S.J. (1985). **Encycl Polym Sci Eng 2: Biodegradable polymers**. Wiley-Interscience, New York.
- Jiang, W., Liu, CH., Wang, ZG., et al. (1998). Brittle-tough transition in PP/EPDM blends: effects of interparticle distance and temperature. **Polymer**. 39: 3285-3288.
- Jiang, W., Liang, H., and Jiang, B. (1998). Interparticle distance-temperature-strain rate equivalence for the brittle-tough transition in polymer blends. **Polymer**. 39: 4437-4442.
- Jiang, W., Tjong, S.C., and Li, R.K.Y. (2000). Brittle-tough transition in PP/EPDM blends: effects of interparticle distance and tensile deformation speed. **Polymer**. 41: 3479-3482.
- Jiang, W., Yu, D., and Jiang, B. (2004). Brittle-ductile transition of particle toughened polymers: influence of the matrix properties. **Polymer**. 45: 6427-6430.
- Jiang, L., Wolcott, M. P., and Zhang, J. (2006). Study of Biodegradable Polylactide/Poly(butylenes adipate-co-terephthalate) Blends. **Biomacromolecules**. 7: 199-207.
- Khurma, R.J., Rohindra, R.J., and Devi, R. (2005). Miscibility study of solution cast blends of poly(lactic acid) and poly(vinyl butyral). **S. Pac. J. Nat. Sci.** 23.
- Krocshowitz, I. and Jacqueline, I. (1990). **Concise encyclopedia of polymer science and engineering**. New York: John Wiley and Sons, Inc.

- Lee, S. and Lee, J. W. (2005). Characterization and processing of Biodegradable polymer of poly(lactic acid) with poly(butylenes succinate adipate). **Korea-Australia Rheology Journal**. 17: 71-77.
- Li, Y., Iwakura, Y., Zhao, L., and Shimizu, H. (2008). Nanostructured Poly(vinylidene fluoride) Materials by Melt Blending with Several Percent of Acrylic Rubber. **Macromolecules**. 41: 3120-3124.
- Lu, J., Qiu, Z., and Yang, W. (2007). Fully biodegradable blends of poly(l-lactide) and poly(ethylene succinate): Miscibility, crystallization, and mechanical properties. **Polymer**. 48: 4196-4204.
- Lunt, J. (1998). Large-scale production, properties and commercial applications of polylactic acid polymers. **Polym. Degrad. Stab.** 59: 145-152.
- Margolina, A. and Wu, S. (1988). Percolation model for brittle-tough transition in nylon/rubber blends. **Polymer**. 29: 2170-2173.
- Martin, O. and Avérous, L. (2001). Poly (lactic acid): plasticization and properties of biodegradable multiphase system. **Polymer**. 42: 6209-6219.
- Pan, P., Zhu, B., and Inoue, Y. (2007). Enthalpy Relaxation and Embrittlement of Poly(L-lactide) during Physical Aging. **Macromolecules**. 40: 9664-9671.
- Phinyocheep, P., Saelao, J., and Buzaré, J.Y. (2007). Mechanical properties, morphology and molecular characteristics of poly(ethylene terephthalate) toughened by natural rubber. **Polymer**. 48: 5702-5712.
- Lee, S. and Lee, J. W. (2005). Characterization and processing of Biodegradable polymer blends of poly(lactid acid) with poly(butylene succinate adipate). **Korea-Australia Rheology Journal**. 17: 71-77.

- Sarasua, J. R., Prud'homme, R. E., Wisniewski, M. Borgne, A. L., and Spassky, N. (1998). Crystallization and melting behavior of polylactides. **Macromolecules**. 31: 3895-3905.
- Sundararaj, U. and Macosko, C. W. (1995). Drop breakup and coalescence in polymer blends: The effect of concentration and compatibilization. **Macromolecules**. 28: 2647-2557.
- Taylor, G.I. (1932; 1934) **Proc. Roy. Soc.** A146, p.339: A138, 41: A146, 501.
- Todo, M., Park, S. D., Takayama, T., and Arakawa, K. (2007). Fracture micromechanisms of bioabsorbable PLLA/PCL polymer blends. **Eng Fract Mech**. 74: 1872-1883.
- Tsuji, H. and Ikada, Y. (1995). Properties and morphologies of poly(L-lactide):1. Annealing condition effects on properties and morphologies of poly(L-lactide). **Polymer**. 36: 2709-2716.
- Van der Wal, A. and Gaymans, R.J. (1999). Polypropylene-rubber blends: 3. The effect of the test speed on the fracture behaviour. **Polymer**. 40: 6045-6055.
- Vert, M., Schwach, G., and Coudane, J.J. (1995). **Macromol Sci-Pure Appl Chem**. A32: 787.
- Walker, I. and Collyer, A.A. (1994). Rubber toughening mechanisms in polymeric materials. **Rubber Toughened Engineering Plastics**. CHAPMAN & HALL.
- Wu, S. (1985). Phase structure and adhesion in polymer blends: A criterion for rubber toughening. **Presented in part at the 16th Europhysucs Conference on Macromolecular Physics**. Brugge, Belgium, 4-7 1984.
- Wu, S. (1987). **Polym. Eng. Sci**. 27: 335.
- Wu, S. (1990). **Polymer**. 31: 972-974.

APPENDIX A

RESULTS OF DISTRIBUTION OF NR PARTICLE SIZE

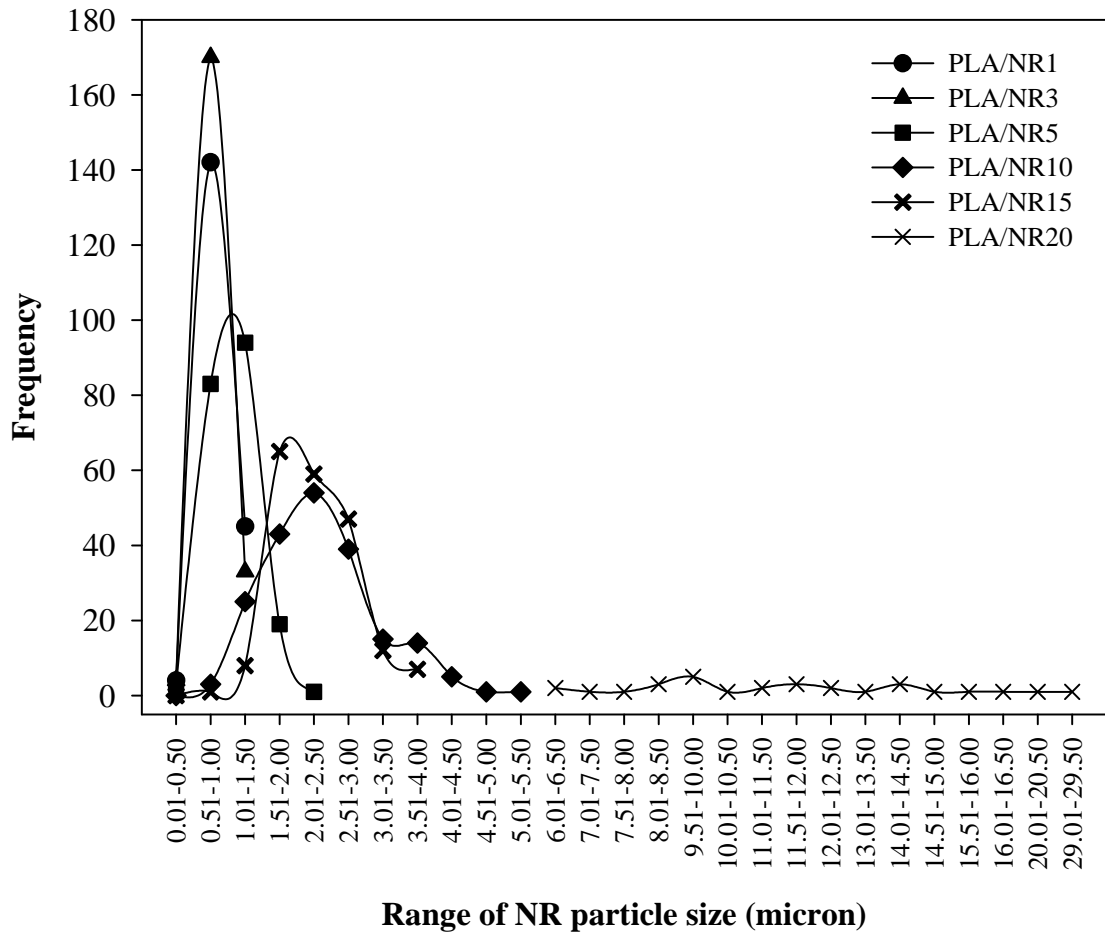


Figure A1 Distribution of NR particle size with different NR contents.

APPENDIX B

PUBLICATION

PHYSICAL STUDY ON TOUGHENING OF POLYLACTIC ACID WITH NATURAL RUBBER

P. Somdee^{1,2}, B. Suksut^{1,2} and C. Deeprasertkul^{1,2*}

¹School of Polymer Engineering, Institute of Engineering,

Suranaree University of Technology, Nakhon Ratchasima 30000, Thailand.

²Center of Excellence for Petroleum, Petrochemicals, and Advanced Materials,

Chulalongkorn University, Bangkok 10330, Thailand

*E-mail: chantima@sut.ac.th, Tel: +66-44-224434

Abstract: This study aims to improve the toughness of polylactic acid (PLA) with natural rubber (NR). Due to their biodegradability, both PLA and NR are of interest. Biodegradable blends of PLA and NR were prepared at various concentrations (5-20 %wt NR content) by melt blending in an internal mixer. Mechanical, thermal properties and phase morphology of the blends were investigated. The percent elongation at break (%) and tensile toughness of PLA/NR blends increased with concentration of NR up to 10 %wt/wt while tensile strength and Young's modulus decreased. At 90/10 %wt/wt PLA/NR, elongation at break is 20.13% and tensile toughness is 499 MPa, which are higher than those of pure PLA, 9.30% and 317 MPa. In agreement with tensile results, impact strength of this blend composition increases three fold (to 6.50 kJ/m²) compared to pure PLA. Beyond 10%wt NR content, both tensile and impact properties decreased. Morphological examination by scanning electron microscopy (SEM) of impact fracture surface showed spherical rubber particles evenly disperse in PLA matrix up to 10%wt NR content. The average particle size of NR (ranging from <1 μm to ~10 μm) increased with the NR content. From differential scanning calorimetry (DSC) analysis, the glass transition temperature (T_g), crystallization temperature (T_c) and the corrected crystallinity of PLA in PLA/NR blends do not change with addition of rubber. The results indicate that toughness improvement of PLA is mainly contributed by NR content and particle size.

Introduction

Poly(lactic acid) (PLA) is a biodegradable polymer that has been widely used in industrial applications. It is a linear aliphatic polyester which can be synthesized by condensation and ring opening polymerization. Commercially available high molecular weight PLA resin is produced by ring opening polymerization of lactides which are the cyclic dimers of lactic acids [1,2]. PLA has high modulus and strength, but is brittle [3]. Blending with other polymers is commonly used to improve its brittleness.

Many studies on incorporation of both biodegradable and non-biodegradable polymer into PLA for toughness improvement have been reported [4-7]. However, rubbers are always considered as the best candidate for toughening. Various factors such as the molecular weight, the crystallinity of the matrix, type and content of the disperse phase, interfacial

characteristic and particle size play important roles on the level of toughening. For example, impact strength of blends can be improved with increasing rubber content in polymer blends [4,5,8]. Rubber phases dispersed in polymer matrix with most particle size less than 100 nm significantly increased toughness of blends even at very small rubber content (<5%) [9]. In addition to toughness, the incorporation of other polymers also affected crystallization of PLA [5,8]. By adding poly(vinyl butyral) (PVB), degree of crystallinity (X_c) of PLA did not change while crystallization rate increased [10]. The presence of poly(butylene succinate adipate) (PBSA) could decrease X_c of PLA [8].

In this study, natural rubber (NR) was chosen for toughening PLA. Besides its high toughness, NR is a biodegradable polymer that is obtained from renewable resource. Mechanical, thermal properties and morphology of pure PLA and PLA/NR blends were investigated.

Materials and Methods

Material: Commercially available PLA (NatureWorks PLA 4042D) was used. From DSC analysis, its glass transition temperature and melting temperature are 52.14°C and 146.68°C, respectively. High ammonia natural rubber (NR) latex was purchased from Thai Hua Rubber Public Company Ltd., Thailand. NR latex was dried at 70°C in an oven before use.

Sample Preparation: An internal mixer (Haake Rheomix 600p) was employed to mix PLA and NR using a rotor speed of 50 rpm at 180°C. Before mixing, dried rubber and PLA pellets were dried in an oven at 70°C for 8 h. The samples for tensile and impact testing were prepared by compression molding (Gotech model GT-7014-A30).

Thermal properties: Differential scanning calorimetry (DSC, Perkin Elmer model DSC-7) was used for determining thermal properties of the sample. All samples were heated from 25 to 200°C at 10°C/min (first heating) and kept isothermal for 2 min to erase previous thermal history. They were then cooled from 200°C to 25°C at 10°C/min and heated to 200°C again at the rate of 10°C/min (second heating).

Mechanical properties: Tensile testing samples were prepared by compression molding. Tensile testing was performed according to ASTM 638 using universal testing machine (UTM, Instron model 5569). The test was conducted with a crosshead speed of 1 mm/min at 25°C.

Notched Izod impact test was performed according to ASTM 256 using an Atlas testing machine (model BPI). Before testing, all specimens were notched.

Morphological characterization: Morphology of the impact fractured surface of pure PLA and PLA/NR blends was characterized using scanning electron microscope (SEM, JEOL model JSM 6400). The samples were coated with gold for 4 min before analysis.

Results and Discussion

Thermal Analysis: DSC second heating thermograms of pure PLA and PLA/NR blends are shown in Figure 1. For pure PLA, the glass transition temperature was found at 52.14°C. The cold crystallization temperature (T_{cc}) appeared at 116.06°C. The double-peak melting temperature (T_m) was observed. Sarasua et al. studied and explained that the melting peak at higher temperature (T_{m2}) belongs to more perfect crystalline structure than that at lower temperature (T_{m1}). The less perfect crystals have enough time to melt and reorganize into crystals with higher structure perfection and remelt at higher temperature [11]. The incorporation of NR did not affect the glass transition of PLA. The T_{cc} was broadened. The T_{m2} peak of the blends was clearly seen and became comparable to the T_{m1} peak as NR content increased.

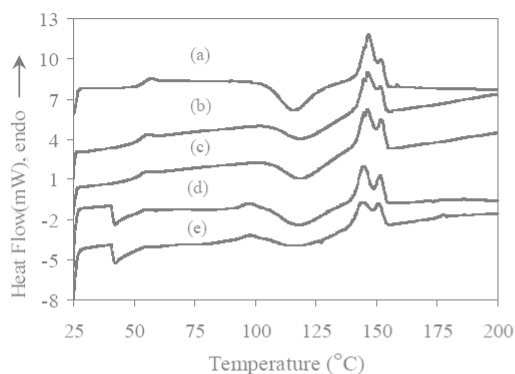


Figure 1. DSC thermograms of PLA/NR blends at heating rate of 10°C/min. Data from the second heat; (a) 0%NR, (b) 5%NR, (c) 10%NR, (d) 15%NR and (e) 20%NR.

The data from the DSC thermograms are summarized in Table 1. The X_c (%) of PLA in the blend was calculated using the following equation:

$$X_c = \frac{100 \times (\Delta H_{m,PLA} - \Delta H_{c,PLA})}{93 \times \Phi_{PLA}}$$

where $\Delta H_{m,PLA}$ is enthalpy of fusion of PLA (J/g), $\Delta H_{c,PLA}$ is enthalpy of crystallization of PLA (J/g), Φ_{PLA} is weight fraction of PLA in blend and enthalpy of fusion of a 100% crystalline PLA is 93 (J/g) [5]. The NR content did not significantly affect the degree of crystallinity. These results suggest that the perfection of PLA crystalline structure can be induced by NR without interfering the crystallinity.

Table 1. Thermal properties of pure PLA and PLA blends.

NR content (wt%)	T_g (°C)	T_{cc} (°C)	T_m (°C)		X_c (%)
			T_{m1}	T_{m2}	
0	52.14	116.06	146.68	151.87	58.76
5	53.31	118.55	146.34	151.69	52.73
10	54.40	118.39	146.17	152.03	57.43
15	54.99	118.14	144.76	151.45	58.68
20	54.58	117.31	144.93	150.96	59.13

Mechanical analysis: Tensile stress-strain curves of pure PLA and blends are shown in Figure 2. Tensile strength is 57 MPa and percent elongation at break is about 9.3% for pure PLA. Tensile strength decreased with increasing NR content. Young's modulus and elongation at break (%) as a function of NR content are shown in Figure 3. Modulus tends to decrease with rubber. Elongation at break increased with NR content up to 10%wt.

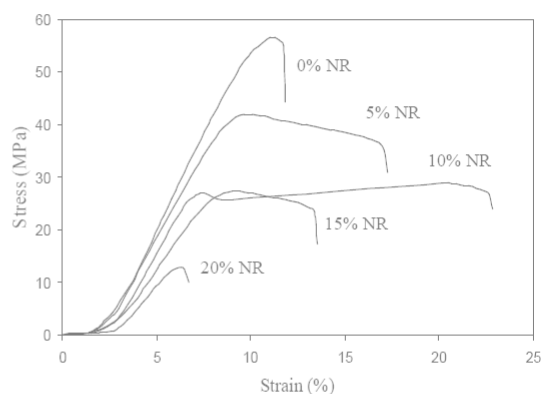


Figure 2. Tensile stress-strain curve of the PLA blends with different NR contents.

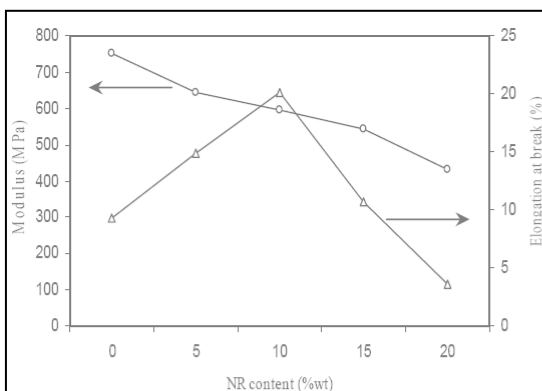


Figure 3. Tensile modulus and elongation at break of PLA blends with different NR contents.

Tensile toughness of PLA blends is also maximum at 10 % wt of NR content as shown in Figure 4. Toughness value of pure PLA is 317 MPa and 10 %wt of NR content is 499 MPa. From tensile results, the optimum NR content for toughening PLA/NR is at 10%wt NR.

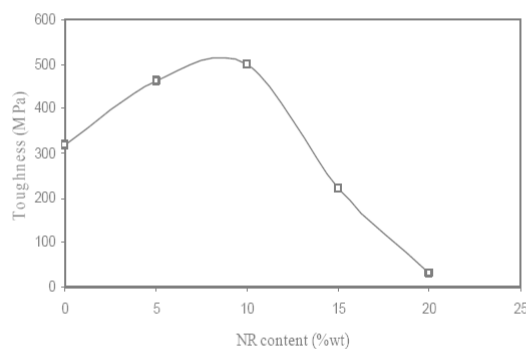


Figure 4. Tensile toughness of PLA blends with different NR contents.

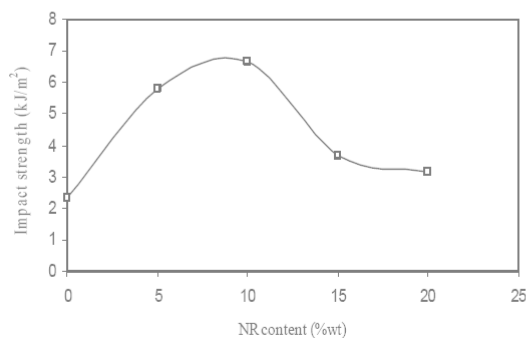


Figure 5. Impact strength of PLA blends with different NR contents.

Impact results are shown in Figure 5. The blend with 10%wt rubber showed maximum impact strength (6.50 kJ/m^2), consistent with the tensile results. Impact strength of this blend composition increases three folds compared to that of pure PLA.

Morphological analysis: SEM micrographs of impact fractured surfaces are shown in Figure 6. It is seen that fractured surface showed spherical rubber particles evenly dispersed in PLA matrix up to 10%wt NR content. When the NR content increased, the average particle size of NR increased ($1.19 \mu\text{m}$ at 5 %wt NR to $2.19 \mu\text{m}$ at 10 %wt NR). Beyond 10%wt NR, coalescence of NR particles was observed (not shown here). These SEM results indicate that the toughness improvement of PLA when adding NR be due to NR content and size. With evenly dispersed rubber particles, the fracture energy can be effectively dissipated.

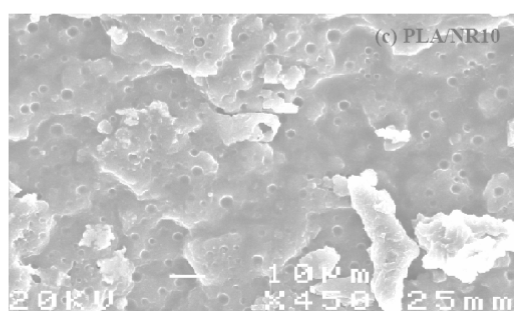
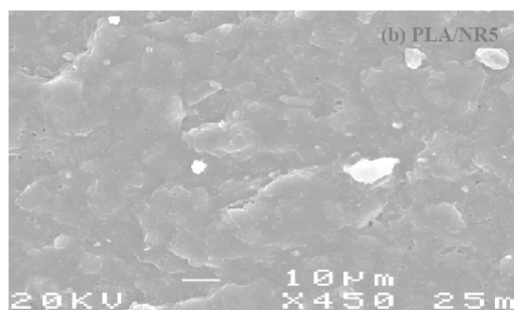
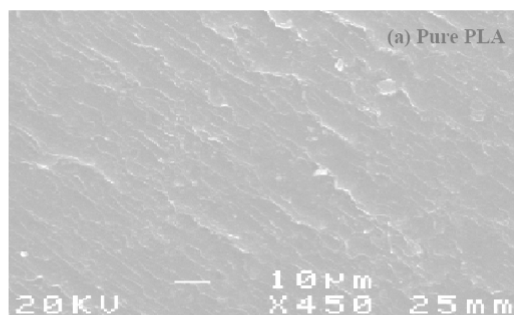


Figure 6. SEM micrographs of PLA/NR blends in the impact testing. (a) Pure PLA (b) PLA-5%NR and (c) PLA-10%NR.

Conclusions

PLA and NR were melt blended. The presence of NR did not affect thermal properties of PLA. Tensile strength and Young's modulus of PLA blends decreased with NR content. Percent elongation at break and impact strength increased with NR content up to 10%wt NR. The SEM results indicated that toughness improvement of PLA is mainly contributed by NR content and particle size.

Acknowledgment

This work was financially supported by the National Research Council of Thailand and Suranaree University of Technology. PS and BS are grateful to the Center of Excellence for Petroleum, Petrochemicals, and Advanced Materials, Chulalongkorn University for scholarships.

References

- [1] R. Auras, B. Harte and S. Selke, *Macromol. Biosci.* **4** (2004), pp. 835-864.
- [2] D. Garlotta, *J. Polym. Environ.* **9** (2001), pp. 63-84.
- [3] C. Keith Riew and Anthony J. Kinloch, Editors, *Toughened plastics I; science and engineering*, American Chemical Society, Washington, DC (1993).
- [4] A. Bhatia and K. Rahul, *Korea-Australia Rheology Journal.* **19** (2007), pp. 125-131.
- [5] M. Todo, S.D. Park, T. Takayama et al., *Engineering Fracture Mechanics.* **74** (2007), pp. 1872-1883.
- [6] L. Jiang and M.P. Wolcott, *Biomacromolecules,* **7**(2006), pp. 199-207.
- [7] J. Lu, Z. Qiu and W. Yang, *Polymer.* **48**(2007), pp. 4196-4204.
- [8] S. Lee and J.W. Lee, *Korea-Australia Rheology Journal.* **17**(2005).
- [9] Y. Li, Y. Iwakura, L. Zhao et al., *Macromolecules.* **41**(2008), pp. 3120-3124.
- [10] J.R. Khurma, D.R. Rohindra and R. Devi, *The South Pacific Journal of Natural Science.* **23**(2005).
- [11] J.R. Sarasua, R.E. Prod'homme, M. Wisniewski, A.L. Borgne, N. Spassky, *Macromolecules,* **31**(1998), pp. 3895-3950.

BIOGRAPHY

Miss Patcharaporn Somdee was born on August 20, 1983 in Ubonratchathani Province, Thailand. In 2006, she graduated in Bachelor's degree from department of Chemical Engineering, faculty of Engineering at Khon Kaen University (KKU) in Khon Kaen Province. Topic of senior project during her Bachelors' degree was **“The Production of Essential Oil by Steam Distillation”**. Then, she continued in field of Polymer Engineering at School of Polymer Engineering, Institute of Engineering at Suranaree University of Technology (SUT) in Nakhonratchasima Province. During her Master's degree study, she presented one poster entitle of **“Physical Study on Toughening of Polylactic Acid with Natural Rubber”** in Pure and Applied Chemistry International Conference 2009 (PACCON 2009) in Phitsanulok Province, Thailand.